Molecular Phylogenetics and Evolution 126 (2018) 250–265

Contents lists available at ScienceDirect

Molecular Phylogenetics and Evolution

journal homepage: www.elsevier.com/locate/ympev

Population genetics, phylogenomics and hybrid speciation of *Juglans* in China determined from whole chloroplast genomes, transcriptomes, and genotyping-by-sequencing (GBS)

Peng Zhao[a,*,1], Hui-Juan Zhou[a,1], Daniel Potter[c], Yi-Heng Hu[a], Xiao-Jia Feng[a], Meng Dang[a], Li Feng[a], Saman Zulfiqar[a], Wen-Zhe Liu[a], Gui-Fang Zhao[a], Keith Woeste[b,*]

[a] *Key Laboratory of Resource Biology and Biotechnology in Western China, Ministry of Education, College of Life Sciences, Northwest University, Xi'an, Shaanxi 710069, China*

[b] *USDA Forest Service Hardwood Tree Improvement and Regeneration Center (HTIRC), Department of Forestry and Natural Resources, Purdue University, 715 West State Street, West Lafayette, IN 47907, USA*

[c] *Department of Plant Sciences, University of California, Davis, CA 95616, USA*

ARTICLE INFO

Keywords:
Juglans
Hybridization speciation
Phylogeography
Gene introgression
Population genetic

ABSTRACT

Genomic data are a powerful tool for elucidating the processes involved in the evolution and divergence of species. The speciation and phylogenetic relationships among Chinese *Juglans* remain unclear. Here, we used results from phylogenomic and population genetic analyses, transcriptomics, Genotyping-By-Sequencing (GBS), and whole chloroplast genomes (Cp genome) data to infer processes of lineage formation among the five native Chinese species of the walnut genus (*Juglans,* Juglandaceae), a widespread, economically important group. We found that the processes of isolation generated diversity during glaciations, but that the recent range expansion of *J. regia*, probably from multiple refugia, led to hybrid formation both within and between sections of the genus. In southern China, human dispersal of *J. regia* brought it into contact with *J. sigillata*, which we determined to be an ecotype of *J. regia* that is now maintained as a landrace. In northern China, walnut hybridized with a distinct lineage of *J. mandshurica* to form *J. hopeiensis*, a controversial taxon (considered threatened) that our data indicate is a horticultural variety. Comparisons among whole chloroplast genomes and nuclear transcriptome analyses provided conflicting evidence for the timing of the divergence of Chinese *Juglans* taxa. *J. cathayensis* and *J. mandshurica* are poorly differentiated based our genomic data. Reconstruction of *Juglans* evolutionary history indicate that episodes of climatic variation over the past 4.5 to 33.80 million years, associated with glacial advances and retreats and population isolation, have shaped Chinese walnut demography and evolution, even in the presence of gene flow and introgression.

1. Introduction

Walnuts and butternuts (*Juglans*) are known for their edible nuts and high-quality wood (Manning, 1978; Aradhya et al., 2007). The genus *Juglans* includes about 21 species distributed in Asia, southern Europe, North America, Central America, western South America, and the West Indies (Manning, 1978; Stanford et al., 2000; Aradhya et al., 2007). Species of *Juglans* are diploid, with a karyotype of 2n = 2x = 32 (Woodworth, 1930). All *Juglans* are monoecious, wind-pollinated, temperate deciduous trees (Manning, 1978). *J. regia* (Common walnut), *J. sigillata* (Iron walnut), *J. cathayensis* (Chinese walnut), *J. hopeiensis* (Ma walnut), and *J. mandshurica* (Manchurian walnut) grow in China (Manning, 1978; Aradhya et al., 2007). Chinese *Juglans* species are divided into two sections (sect. *Dioscaryon*, and sect. *Cardiocaryon*) based on species' geographical distribution, leaf, flower, and fruit morphology (Manning, 1978) and molecular evidence (Fjellstrom and Parfitt, 1995; Stanford et al., 2000; Aradhya et al., 2007). *J. regia* and *J. sigillata* belong to sect. *Dioscaryon*, and the other three species (*J. cathayensis*, *J. hopeiensis*, and *J. mandshurica*) belong to sect. *Cardiocaryon* (Stanford et al., 2000; Aradhya et al., 2007). Phylogeny based on complete chloroplast genomes, protein coding sequences (CDS), and the introns and spacers (IGS) data (Hu et al., 2017) strongly supported division of the five Chinese walnut species into two previously recognized sections (*Juglans/Dioscaryon* and *Cardiocaryon*) with a 100%

* Corresponding authors at: College of Life Sciences, Northwest University, North Taibai Road 229, Xi'an, Shaanxi 710069, China (P. Zhao).
E-mail addresses: pengzhao@nwu.edu.cn (P. Zhao), kwoeste@fs.fed.us, woeste@purdue.edu (K. Woeste).
[1] These authors contributed equally to this work.

https://doi.org/10.1016/j.ympev.2018.04.014
Received 28 May 2017; Received in revised form 27 March 2018; Accepted 9 April 2018
Available online 18 April 2018
1055-7903/

Table 1
Sources of five Chinese *Juglans* taxa sampled for genetic analyses and their chloroplast haplotypes.

Taxon	Population	Location	Longitude (E)	Latitude (N)	Individuals/(Hap)
Juglans regia	BJ	Baoji, Shaanxi	107°32′56″	34°13′08″	5/1 (H13)
Juglans regia	CL	Zhangjiajie, Hunan	111°14′29″	29°25′37″	4/1 (H13)
Juglans regia	DHY	Maofeng, Beijing	115°17′10″	39°29′45″	3/0 (ND)
Juglans regia	FJ	Shigui, Chongqing	106°33′05″	29°33′46″	2/1(H12)
Juglans regia	GS	Tianshui, Gansu	104°52′48″	34°43′12″	5/1 (H12)
Juglans regia	GZ	Zunyi, Guizhou	106°47′35″	27°18′18″	2/1 (H12)
Juglans regia	HG	Honghegu, Shaanxi	116°34′12″	37°19′48″	4/0(ND)
Juglans regia	HH	Heihe, Shaanxi	108° 0′42″	33°52′24″	5/0 (ND)
Juglans regia	HN	Nanyang, Henan	112°13′11″	33°14′47″	3/1 (H12)
Juglans regia	PHT	Pingli, Shaanxi	109°16′29″	32°20′57″	3/1(H16)
Juglans regia	SCN	Emei, Sichuan	103°31′21″	29°35′28″	4/0(ND)
Juglans regia	SD	Dezhou, Shandong	116°34′12″	37°19′48″	4/1 (H14)
Juglans regia	SXL	Qinshui, Shanxi	113°00′10″	35°26′10″	3/1(H12)
Juglans regia	XJ	Akesu, Xinjiang	82°57′43″	41°43′04″	4/1(H12)
Juglans regia	XJH	Bamang, Xinjiang	86°47′36″	42°01′11″	5/1 (H12)
Juglans regia	XJM	Bazhou, Xinjiang	87°19′27″	42°12′5″	4/0 (ND)
Juglans regia	YC	Yichang, Hubei	111°14′23″	30°37′40″	3/0(ND)
Juglans regia	YKD	Chengde, Hebei	118°29′07″	40°36′41″	2/0 (ND)
Juglans sigillata	BS	Baoshan, Yunan	99°42′00″	24°54′27″	2/1 (H12)
Juglans sigillata	LJ	Lijiang, Yunnan	100°03′41″	26°54′21″	4/1(H15)
Juglans sigillata	PKM	Puer, Yunnan	100°57′38″	22°53′58″	2/1 (H12)
Juglans sigillata	THC	Liupanshui, Guizhou	104°47′52″	26°34′06″	2/1 (H12)
Juglans sigillata	TKM	Kunming, Yunnan	102°53′36″	24°51′48″	3/1(H12)
Juglans sigillata	ZY	Linzhi, Xizang	94°25′10″	29°59′22″	1/1 (H12)
Juglans cathayensis	BGY	Baoji, Shaanxi	107°44′41″	34°05′28″	4/1(H1)
Juglans cathayensis	BX	Baoxing, Sichuan	102°42′39″	30°20′42″	3/1 (H5)
Juglans cathayensis	BXS	Baxianshan, Tianjin	116°43′05″	39°30′18″	1/0(ND)
Juglans cathayensis	HP	Huping, Hunan	111°29′14″	29°33′51″	4/1 (H3)
Juglans cathayensis	MLS	Shigui, Chongqing	106°33′05″	29°33′46″	1/0(ND)
Juglans cathayensis	PYHT	Pingli, Shaanxi	109°09′44″	32°16′01″	2/1 (H2)
Juglans cathayensis	SMX	Sanmenxia, Henan	111°24′32″	34°30′38″	1/0 (ND)
Juglans cathayensis	SNJ	Shennongjia, Hubei	110°18′32″	31°35′31″	4/1 (H4)
Juglans cathayensis	YBJ	Tianshui, Gansu	106°42′56″	34°14′60″	2/0 (ND)
Juglans cathayensis	YCL	Zhangjiajie, Hunan	111°14′29″	29°25′37″	1/0 (ND)
Juglans cathayensis	YJG	Xinyang, Henan	114°05′32″	31°52′38″	1/0 (ND)
Juglans cathayensis	YKM	Kunming, Yunnan	102°36′39″	24°33′18″	3/0 (ND)
Juglans cathayensis	YLT	Lantian, Shaanxi	109°19′12″	34°09′00″	1/0 (ND)
Juglans cathayensis	YLL	Shiyan, Hubei	110°10′43″	31°54′45″	3/1 (H6)
Juglans cathayensis	ZQ	Zhuque, Shaanxi	108°32′51″	33°49′56″	1/0 (ND)
Juglans mandshurica	CBS	Changbaishan, Jilin	127°57′48″	42°05′04″	3/1 (H9)
Juglans mandshurica	HEB	Haerbin, Heilongjiang	127°22′33″	45°29′36″	6/2 (H9)
Juglans mandshurica	LN	Dandong, Liaoning	124°09′36″	40°18′18″	1/1 (*H*11)
Juglans mandshurica	XLM	Xiaolongmeng, Beijing	115°35′05″	39°56′11″	6/2 (H9,10)
Juglans hopeiensis	KC	Kuancheng, Hebei	118°22′48″	40°36′10″	3/1 (*H*10)
Juglans hopeiensis	LS	Laishui, Heibei	115°35′35″	39°29′36″	5/1(H9)
Juglans hopeiensis	XK	Xiakou, Beijing	116°10′32″	40°16′10″	2/1(H8)
Juglans hopeiensis	XL	Xinglong, Heibei	117°29′01″	40°22′15″	2/1 (H7)
Juglans hopeiensis	XM	Xiaolongmen, Beijing	115°35′05″	39°56′11″	1/1 (H9)
					140/34

bootstrap (BS) support. The native range of common walnut is uncertain, but (apparently) wild populations grow in often isolated favorable habitats across a wide geographical range from China to the Iberian Peninsula (Manning, 1978; Draine and Hiden 1998; Martínez-García et al., 2016; Pollegioni et al., 2017). *J. regia* is native to the mountainous regions of central Asia (Pollegioni et al., 2015; Martínez-García et al., 2016), while Iron walnut (*J. sigillata*) is indigenous to China, distributed mainly in southwestern China (Wang et al., 2015) sympatric with *J. regia*. *J. cathayensis* is widely distributed in southern China (Bai et al., 2014), while *J. mandshurica* is mainly distributed in North China, Northeast China and the Korean Peninsula (Wang et al., 2016). *J. hopeiensis* is narrowly distributed in northern China in the hilly, mid-elevation area between Hebei province, Beijing, and Tianjin (Hu et al., 2015). A strongly supported phylogeny of these five species is not available due to a lack of informative molecular markers (Fjellstrom and Parfitt, 1995; Stanford et al., 2000; Aradhya et al., 2007). Studies of gene flow and introgression have concluded *J. regia* and *J. sigillata* are particularly closely related, and some have questioned whether they are distinct (Wang et al., 2008; Wang et al., 2015). Aradhya et al. (2007) used ITS, RFLP, and cpDNA sequence data to suggest *J. regia* and *J. sigillata* are distinct species. Grimshaw (2003) considered *J. sigillata* distinct and valid based on morphology.

The relationships among species of sect. *Cardiocaryon* are unsettled. For example, the relationship of Ma walnut (*J. hopeiensis*) to other members of the section *Cardiocaryon*, especially *J. mandshurica* (Lu et al., 1999; Aradhya et al., 2007) is disputed. Although the previous phylogenetic study concluded Ma walnut is a well-defined lineage and a sister clade to *J. ailantifolia*, *J. mandshurica* and *J. cathayensis* within section *Cardiocaryon* (Stanford et al., 2000; Aradhya et al., 2007), evidence from randomly amplified polymorphic DNA (RAPD) markers, isozymes, and karyotype analysis indicated that *J. hopeiensis* might have arisen from the recent hybridization of *J. regia* and *J. mandshurica* (Wu et al., 1999; Mu et al., 1990). Grimshaw (2003) considered *J. hopeiensis* and *J. cathayensis* to be synonyms of *J. mandshurica*. *J. cathayensis* and *J. mandshurica* were also combined into one species in Flora of China (English version) (Lu et al., 1999), which does not consider *J. hopeinesis* (Kuang and Lu 1979; Aradhya et al., 2007) a valid taxon. Others have suggested that *J. hopeiensis* is a variant of *J. mandshurica* based on another characteristics and morphology (Lu et al., 1999). Several important studies have drawbacks/shortages in sampling because their authors

did not have access to adequate samples of all Chinese *Juglans* (Fjellstrom and Parfitt, 1995; Stanford et al., 2000; Aradhya et al., 2007).

There are many potential advantages to using datasets that span entire nuclear and chloroplast genomes (Cp genome) to sort out phylogeny and evolutionary history (McCormack et al., 2013; Stölting et al., 2015; Daniell et al., 2016). Large, genome-scale datasets can be used to address phylogenetic relationships among closely related species and, at the same time, examine patterns of lineage sorting and historical hybridization (Escudero et al., 2014; Dodsworth et al., 2015; Daniell et al., 2016). The uniparental inheritance (maternal transmission), haploid state, and general absence of recombination of the Cp genome (limiting gene flow to seed dispersal only, Moore et al., 2010) make Cp genome sequences particularly useful for studies of plant population genetic and phylogeography (Perdereau et al., 2017). Analysis of genetic variability within the nuclear genome using orthologous genes and Genotyping-by Sequencing (GBS) has the potential to resolve divergence that straddles the population-species boundary (Davey et al., 2011; Nicotra et al., 2016; Mattila et al., 2012; Yang et al., 2014).

Here, we use population genomic approaches to clarify the evolutionary relationships among the five Chinese *Juglans* species and to gain insight into intraspecific variation within each of the two sections of *Juglans* native to China (Stanford et al., 2000; Aradhya et al., 2007). Other aims include to determine the nature and extent of gene flow between sect. *Dioscaryon* and sect. *Cardiocaryon* and its consequences, and to determine the relationship between *J. regia* and *J. sigillata*. Finally, we wanted to determine if *J. hopeiensis* arose from a recent hybridization and, if so, how and when this event occurred.

2. Materials and methods

2.1. Sample collection, DNA extraction, and RNA extraction

For whole chloroplast genome (Cp genome) research, fresh leaves of 34 healthy tree of five *Juglans* species were collected from different locations in China (eleven *Juglans regia*, six *J. sigillata*, five *J. hopeiensis*, six *J. cathayensis*, and six *J. mandshurica*, Table 1) and silica gel-dried and stored at −4°C. High-quality genomic DNA was extracted using a modified CTAB method (Zhao and Woeste, 2011). For transcriptome research, fresh leaves, buds, flowers were collected from single, mature, healthy-appearing *J. regia* (Qinling Mountains), *J. sigillata* (Yunnan province), *J. hopeiensis* (Laishui, Beijing), *J. cathayensis* (Qinling Mountains), and *J. mandshurica* (Xiaolongmen, Beijing) and immediately frozen in liquid nitrogen prior to storage at −80 °C. Total RNA was extracted using a Plant RNA Kit (OMEGA Bio-Tek, Norcross, GA, USA). RNA degradation and contamination was monitored on 1% agarose gels (details see Hu et al., 2017).

For Genotyping by sequencing (GBS), five Chinese walnut (*Juglans*) species were collected from field sites across their biological ranges (Table 1). A total of 140 individuals (65 *Juglans regia*, 13 *J. sigillata*, 14 *J. hopeiensis*, 32 *J. cathayensis*, and 16 *J. mandshurica*) from 47 locations (18 populations of *J. regia*, 5 populations of *J. sigillata*, 5 populations of *J. hopeiensis*, 15 populations of *J. cathayensis*, and 4 populations of *J. mandshurica*) were collected for analysis (Table 1). Each sampled tree was a mature adult, apparently healthy, growing in a mountain forest, along a forest road, or near a village but not in an orchard or on farmed land. Sampled trees were separated by at least 100 m. Sampled locations were mapped using ArcGIS (version 10. 0; ESRI, 2010) (Fig. 1). Fresh leaves were dried with silica gel prior to DNA extraction. DNA was extracted following the methods described by Doyle and Doyle (1987) and Zhao and Woeste (2011). The DNA was quantified and its quality evaluated using three methods: (i) Agarose gel electrophoresis to test DNA purity and integrity, (ii) Nanodrop (Wilmington, DE, USA) test DNA purity (OD260/OD280), (iii) Qubit® DNA Assay Kit in Qubit® 2.0 Flurometer (Life Technologies, CA, USA) to measure DNA concentration.

2.2. Chloroplast genome sequencing and phylogenetic analysis

We previously sequenced the complete chloroplast genome of *J. regia* with the Illumina HiSeq sequencing platform was performed by Novogene Bioinformatics Technology Co., Ltd., Beijing, China (www.novogene.cn). The complete chloroplast genomes of all samples (Table 1) were sequenced using Illumina HiSeq 2500 and assembled via reference-guided assembly based on the Cp genome of *J. regia* (Hu et al., 2016, NCBI Accession number: KT963008) (Table S1). Raw sequence reads obtained from whole genome sequencing were aligned to the *J. regia* chloroplast genome using Bowtie2 v2.2.6 (Langmead and Salzberg, 2012), and assembled into genomes using aSPAdes v3.6 (Bankevich et al., 2012) assembler. Gaps and boundaries were extended using mitobim v. 1.7 (Hahn et al., 2013) based on mira v. 4 (Chevreux et al., 2004). Haplotype diversity (H_d) and nucleotide diversity (π_s) were calculated using DNASP v.5 (Librado and Rozas, 2009). To generate median-joining (MJ) haplotype networks, all chloroplast genome sequence variation was analyzed using Popart v1.7 (Forster and Ro, 1994; Leigh and Bryant, 2015). Heterozygous bases were removed and sequences were aligned using MAFFT v7.017 (Katoh and Standley, 2013). Statistical selection of a TVM + I substitution model was made using ModelTest v3.7 (Posada and Crandall 1998) and a phylogenetic tree was then estimated using MrBayes v3.2.6 (Ronquist et al., 2012). Run parameters were: a chain length of 1,100,000 and a burn-in length of 100,000 over 4 heated-chains (chain temp 0.2). Phylogenetic analyses of the Cp genome were performed using all five Chinese *Juglans* species, *J. nigra*, *Carya sinensis*, and *Castanea mollissima* (Jansen et al., 2011, NCBI accession number: NC_014674.1) (Details see Hu et al., 2017).

2.3. GBS sequencing and SNP analysis

Genotyping-by-Sequencing (GBS) was performed as described by Elshire et al. (2011) at Novogene Bioinformatics Technology Co., Ltd., Beijing, China (www.novogene.cn). Briefly, genomic DNA from individual samples was digested with *Mse*I and *HaeIII* restriction enzyme. Digested DNA was ligated with one of 96 uniquely barcoded sequencing adaptor pairs (Elshire et al., 2011; Morris et al., 2011). Library amplicons between 250 and 600 bp were extracted from an agarose gel and sequenced in a HiSeq2500-PE125 using a 150 bp Paired End protocol.

The original image data obtained by high throughput sequencers was transformed to raw data that was filtered to good reads containing adapters. The remaining high quality reads were mapped to the walnut reference genome (Martínez-García et al., 2016, http://dendrome.ucdavis.edu/ftp/Genome_Data/genome/Reju/) using BWA v0.7.8 (Li and Durbin, 2009) with the command 'mem-t4-k32-M'. After alignment, we performed SNP calling on a population scale using a Bayesian approach as implemented in the package SAMtools v1.3.1 (Li et al., 2009). We then calculated genotype likelihoods from reads for each individual at each genomic location, and the allele frequencies in the sample with a Bayesian approach. The 'mpileup' command was used to identify SNPs with the parameters as '-q 1 -C 50 -t SP -t DP -m 2 -F 0.002'. Then, to exclude SNP calling errors caused by incorrect mapping or Indels, only high quality SNPs (coverage depth ≥ 2 and ≤ 80 , RMS mapping quality ≥ 20, maf ≥ 0.05, miss ≤ 0.1) were kept for phylogeny analysis. Consequently, 45,548 SNPs were left for further analysis after filter from 4,343,085 raw SNPs.

2.4. Population genetic polymorphism using GBS sequencing data

Phylogenetic analyses were performed on 45,548 SNP loci present in at least half of the individuals we sequenced (but present in all species). After the SNP detection, the individual SNPs were used to calculate the distance among populations. The software TreeBest v1.9.2 was used to calculate the distance matrix, and on this basis, a phylogenetic tree was constructed by neighbor-joining. Guide values

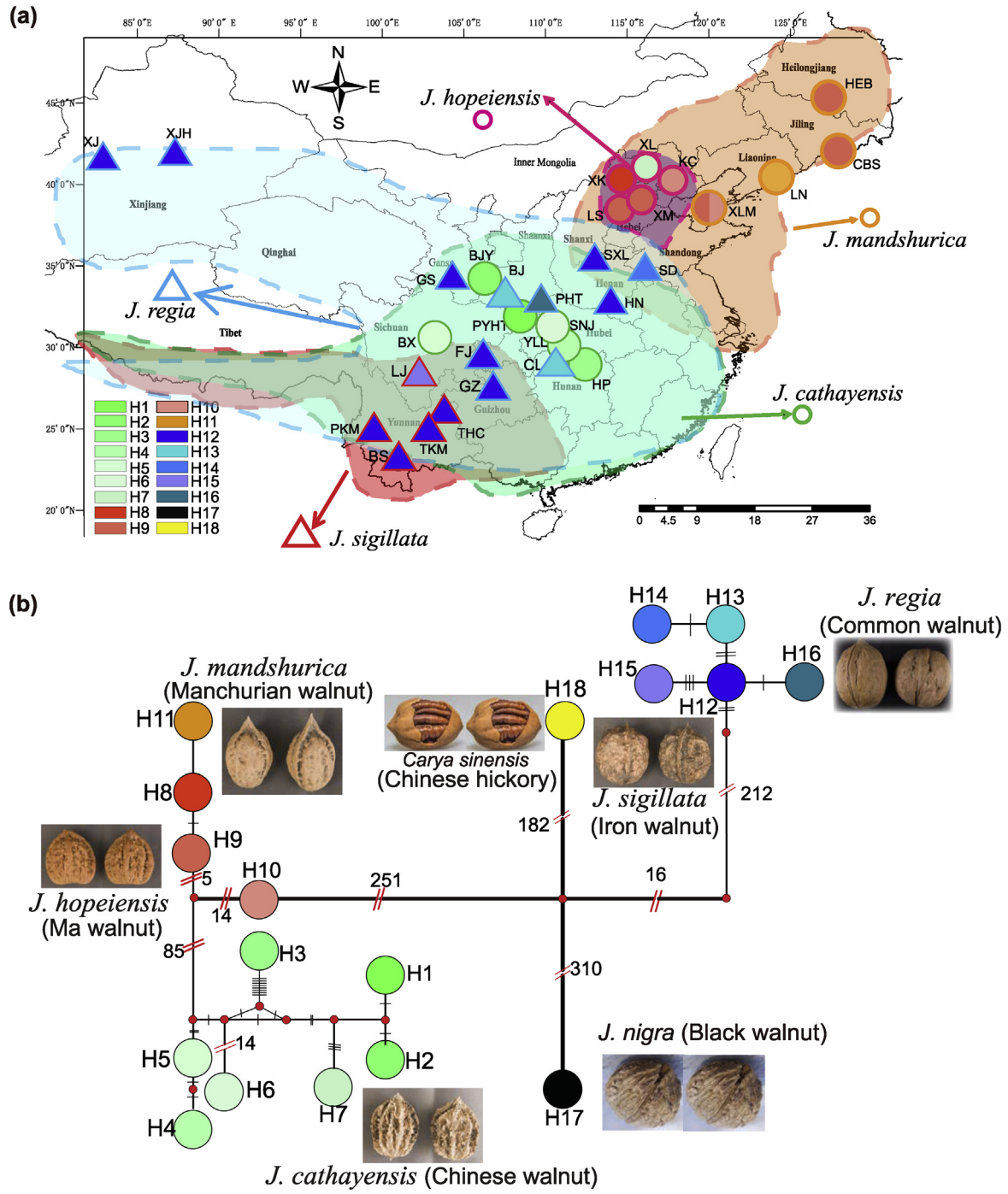

Fig. 1. Species ranges, geographical distribution of haplotypes, and phylogenetic relationship among five Chinese walnut (*Juglans*) taxa. (a) Geographical distribution of 18 chloroplast haplotypes in five Chinese *Juglans* and sampled locations. Shading indicates the native range of each of the five Chinese *Juglans* based on the native distribution of *Juglans* (Aradhya et al., 2007). Colors of haplotypes correspond of those of the small Fig. in the left corner of the map. Haplotypes H9 and H12 are represented using two colors to indicate that *J. hopeiensis* and *J. mandshurica* shared H9, and *J. sigillata* and *J. regia* shared H12. The triangles indicate *J. regia* and *J. sigillata*, circles indicate *J. hopeiensis*, *J. mandshurica*, and *J. cathayensis*. The perimeter color of triangles and circles indicates species. (b) The minimum spanning network of 18 chloroplast genome haplotypes rooted by *Juglans nigra* and *Carya sinensis*. In the network diagram, small red circles indicate intermediate haplotypes not detected in the dataset; red split lines and numbers indicate mutation steps supported by indels, while black lines indicate one mutation step supported by indels. Colors of haplotypes correspond to taxa as indicated in the inset box of Fig. 1a. The yellow (H18) and black circles (H17) indicate the haplotypes of *Carya sinensis* and *J. nigra*, respectively.

(bootstrap values) were calculated more than 1000 times (Li et al., 2006). We also constructed a Maximum Likelihood (ML) phylogenetic tree using all 140 individuals of the five Chinese *Juglans* species (Fig. S4). Based on concatenated SNP sequences, divergence times were estimated by MCMCtree package in PAML 4.5 (Yang, 2007), using soft fossil constraints under various molecular clock models. The time unit was 100 Million years (Mya). We added the calibration of the most recent common ancestor of *Cardiocaryon* and *Rhysocaryon* [0.1, 0.2] (Bai et al., 2016), to edit the tree. The clock variable was set to 2. The process was run to sample 10,000 times using HKY85 as the substitution model, with the sample frequency set to 50 after a burn-in of 50,000 iterations.

2.5. Population structure and principal components analysis

Population genetic structure was analyzed via an expectation maximization algorithm, as implemented in the program FRAPPE v1.170 (http://med.stanford.edu/tanglab/software/frappe.html). This approach involves use of multiple loci GBS data to cluster samples into groups (*K*). The number of genetic clusters/groups, *K*, was tested from 1 to 10 and 20 independent runs with 100,000 burn-in iterations, followed by 500,000 Markov Chain Monte Carlo (MCMC) iterations for each K value. The most likely number of genetic clusters (optimal *K*) was determined using ADMIXTURE (Alexander et al., 2009). Analysis was performed at several different levels of differentiation; we initially used all samples, and then hierarchically tried smaller structure groups consisting of subgroups of species. The principal component analysis (*PCoA*) of 140 samples was performed based on SNPs among individual genomes using GCTA (Yang et al., 2011) and GAPIT software (Lipka et al., 2012).

2.6. Transcriptome sequencing and phylogenetic analysis

Transcriptome sequencing was performed on Illumina HiSeq2000 by Novogene Bioinformatics Technology Co., Ltd., Beijing, China (http://www.novogene.cn). Orthologous groups were constructed from the BLASTP results with OrthoMCL v2.0.9 (Fischer et al., 2011) using default settings and used for the phylogenetic tree reconstruction.

2.7. Ecological niche modeling

Geographical information for the presence of the five Chinese *Juglans* species (*J. regia*, n = 1, 200 individuals; *J. sigillata*, 500 individuals; *J. hopeiensis*, 50 individuals; *J. mandshurica*, 500 individuals; *J. cathayensis*, 600 individuals) was obtained from sampling locations, the distribution records for *J. hopeiensis* sourced from the National Specimen Information Infrastructure (http://www.nsii.org.cn/), and China Virtual Herbarium (http://www.cvh.org.cn/). Ecological niche modeling was employed to provide evidence for the location and extent of habitat for each of the five species during last glacial maximum (LGM, 21 ka BP), the inter-glacial period (LIG, 130 ka BP), and recent past. Species distribution models for all five Chinese walnuts were generated using MAXENT v3.3.3 (Phillips et al., 2006). Prior to modeling, all records were mapped and examined to identify and exclude records with obvious geo-referencing errors and misidentifications.

To explore the potential distribution of five Chinese walnut species under current climatic conditions and predict where suitable conditions were present in the past based on paleoclimate environmental layers, we used 19 biologically meaningful climate variables (BIO1-19, Table S9). The 19 bioclimatic layers were downloaded from WorldClim website at 2.5 arc-min resolution (http://www.worldclim.com). A current distribution model was then projected onto the set of climatic variables simulated 20 times by both the Community Climate System Model (CCSM3.0; Collins et al., 2006) and the Model for Interdisciplinary Research on Climate (MIROC, Otto-Bliesner et al., 2006) to infer the extent of suitable habitat during the last glacial maximum (LGM, 21 ka BP). The paleo-coastlines during the LGM were estimated assuming a 130 m lower sea level. In addition, we projected the model to the last stage of the inter-glacial period (LIG, 130 ka BP) using the climate model of Otto-Bliesner et al. (2006). In order to examine the relative importance of the climate variables on the species distribution, we evaluated percent contribution, permutation importance, and jackknife tests (Ornelas et al. 2016). To assess the degree of ecological niche overlap among *Juglans* species and different lineages, we performed pairwise analyses, examining the niche space between *J. regia*/*J. sigillata*, *J. regia*/*J. hopeiensis*, *J. regia*/*J. mandshurica*, *J. mandshurica*/*J. hopeiensis*, *J. mandshurica*/ *J. cathayensis*, and sub-cluster I of *J. regia* (Northwestern China, Xinjiang province)/ sub-cluster II of *J. regia* (mostly southern and eastern China). We evaluated niche model overlap using Schoener (1968) and Hellinger's *I* calculated in ENMTools (Warren et al., 2010; Dowell and Hekkala, 2016). Schoener's *D* and Hellinger's *I* range from 0 (no overlap) to 1 (complete overlap) (Warren et al., 2008). Significance of niche similarity metrics was tested in ENMTools, assessed with a one-sided Wilcoxon test, and plotted using the ggplot2 package (Wickham, 2009) in R v3.1.3 (R Core Team, 2014).

2.8. Impact of environmental factors on genetic structure (isolation by environment)

In order to evaluate the effect of present climatic conditions on the observed pattern of genetic differentiation, we tested for the relationship between pairwise F_{ST} and climatic distance while controlling for geographic distance for the 47 populations. Nineteen bioclimatic layers for the occurrence points as used earlier in ecological niche modeling (ENM) were summarized into the first two axes of a principal coordinate analyses (*PCoA*) using R 3.1.0. We computed climatic (Euclidian) distance matrices based on population scores for both *PCoA* axes (PC1 and PC2), and for each bioclimatic layers. Tests were performed for the whole data set, including both northern and southern lineages, using partial Mantel tests ('mantel.partial' function; R Core Team 2013) based on 10, 000 permutations.

3. Results

3.1. Sequence assembly and SNP detection

In total, 49.57 GB quality reads of transcriptome were generated, resulting in a total of 46.37 GB of clean data for assembly (Dang et al., 2015, 2016; Hu et al. 2015, 2016, details see Table S2). The mean Q30 percentage (sequencing error rate < 0.05%) ranged from 90.99 to 91.88 across all five species, overall mean Q30 percentage was 91.35. GC percentage ranged from 45.16 to 46.64, mean GC percentage was 45.52 (Table S2). *De novo* assemblies generated 1,039,412 transcripts including 451,242 unigenes. The mean length of the transcripts varied from 1212 bp to 2,577 bp, with an average of 1361 bp, and mean N50 value was 2228 bp. The number of unigenes varied from 81,909 to 103,167 with an average size of 670 bp and mean N50 value of 1186 bp. Full-length coding DNA sequences (CDS) (N = 94,933) longer than 500 bp accounted for about 45.38%. When we aligned the CDS with a threshold of 1e-5 by performing a BLASTX search against diverse protein databases, a total of 43,807 gene families were obtained, including 6421 Core Orthologs (Table S3). When we extracted and aligned the putative CDSs, a total of 190 orthologous unigenes were found and annotated for all five Chinese *Juglans* based on comparison with ten other plant species including *Oryza sativa*, *Glycine* max, *Malus domestica*, *Vitis vinifera*, *Ricinus communis*, *Populus trichocarpa*, *Theobroma cacao*, *Castanea mollissima*, and *Arabidopsis thaliana* (Table S4).

Using GBS, 1179.4 Gb raw reads and 1172.4 Gb clean reads were generated. For each sample, 30,213 high-quality tags were identified from 4.07 G paired-end reads (Table S5). The sequence data was high-quality (Q20 ≥ 90% and Q30 ≥ 85%). The mean GC content was 36.7% (Table S6). A total of 8,095,840 SNPs with an MAF ≥ 0.05 were identified from 47 populations of 140 individuals with a mean of 57,827 SNPs (Table S7) in each of the five Chinese *Juglans*. A total of 45,548 SNPs were identified in the nuclear genomes of Chinese *Juglans* using genotyping by sequencing data.

3.2. Phylogeny analysis using chloroplast genome

The complete plastome sequences of 34 *Juglans* individuals plus *J. nigra* and *Carya sinensis* were aligned; their length averaged 160, 350 bp, containing 1, 849 polymorphic sites, 1, 293 singleton variable sites, and 556 parsimony informative sites (PICs, 0.41%) were detected across five Chinese *Juglans* plus *J. nigra* and *Carya sinensis*. Among the 34 *Juglans* individuals and the outgroup *Carya sinensis* we detected 18

chloroplast haplotypes based on complete genome sequences (Fig. 1); two haplotypes were unique to *J. hopeiensis* (Fig. S1). The haplotype diversity (h_d) and nucleotide diversity (π_s) for all samples were 0.867 and 0.0025, respectively. The 18 haplotypes were highly differentiated among species, but haplotype richness was low across the geographic range within species. Chinese walnut (*J. cathayensis*) contained the highest haplotype diversity. Each individual we sequenced contained a unique chloroplast haplotype (H1, H2, H3, H4, H5, and H6), while *J. mandshurica* had three haplotypes (H9, H10, and H11) (Fig. 1). The statistical parsimony network of 18 chloroplast genome haplotypes showed that two samples of Ma walnut (*J. hopeiensis*) shared haplotype H9 with *J. mandshurica*, while other samples of *J. hopeiensis* contained haplotypes H8 and H7, which were not found in any sample *of J. mandshurica* (Fig. 1). Common walnut (*J. regia*), the most widespread species, only had four haplotypes (H12, H13, H14, and H16) among 11 individuals, while four samples of *J. sigillata* shared haplotype H12 with five *J. regia* individuals (XJ, XJH, GS, BJ, and GZ). One *J. sigillata* sample (LJ) contained a private haplotype (H15) (Fig. 1).

The minimum spanning network of 16 chloroplast genome haplotypes (omitting *J. hopeiensis* haplotypes) clearly separated the sect. *Juglans/Dioscaryon* clade and the sect. *Cardiocaryon* clade, while *J. regia* and *J. sigillata* shared haplotype H12 (Fig. S1). The chloroplast-based phylogeny resolved lineage relationships with high statistical support (> 95%), indicating that there were four clades, one associated with *J. regia* and *J. sigillata* (sect. *Juglans/Dioscaryon* clade), one associated with *J. nigra* (black walnut clade as outgroup), one associated with outgroup *Carya sinensis*, and one associated with *J. mandshurica* and *J. cathayensis* (sect. *Cardiocaryon* clade).

The phylogenetic relationships among the species based on chloroplast sequences were depicted with a divergence time tree (Fig. 2a; Fig. S2). A point estimate for the coalescent time among three *Juglans* chloroplast genome clades was dated to 44.98 Mya/44.99 Mya, while *J. regia* and *J. sigillata* diverged much more recently (0.25 Mya/0.85Mya), and *J. cathayensis* diverged from *J. mandshurica* before 13.46 Mya/15.68 Mya (95% HPD: 5.12–26.52 Mya, Fig. 2a; Fig. S2). The tree topology are strong similar using Maximum likelihood (ML) and Bayesian inference (BI) methods (Fig. 2a, Fig. S2). However, the divergence time estimates between sect. *Juglans/Dioscaryon* and sect. *Cardiocaryon* chloroplasts differed considerably depending on whether estimates of divergence was anchored by the separation of *Juglans* from *Castanea mollissima* versus the separation of *Juglans* from *Carya sinensis*. In the former case, divergence times between species of two sections were estimated at 0.84 Mya (Fig. 2b) versus 36.15 Mya when the anchor was *C. sinensis* (Fig. 2c), while the divergence between the *J. regia* and *J. sigillata* was estimated to have occurred 0.02 Mya (Fig. 2b) versus 0.22 Mya (Fig. 2c). *J. cathayensis* diverged from *J. mandshurica* 0.17 Mya (*C. mollissima* anchor, Fig. 2b) or 23.93 Mya (*C. sinensis*, Fig. 2c) based on whole chloroplast genome sequences.

3.3. Population and phylogenomic analysis by Genotyping-By-Sequencing (GBS) based on 45,548 SNPs

The (nuclear) genome-wide phylogeny clearly resolves the two walnut sections (*Dioscaryon* and *Cardiocaryon*) (Fig. 3; Figs. S3, S4). All phylogenies are congruent and significant and similar to *PCoA* and FRAPPE output (Fig. 3; Figs. S3, S4). Assignment of all individuals from all geographic localities to genetic clusters using FRAPPE revealed an optimum $K = 4$ genetic clusters (Fig. S3). When $K = 4$ genetic clusters (Fig. 3a), *J. cathayensis* and *J. mandshurica* samples were joined into a single cluster, with *J. hopeiensis* clearly admixed. Common walnut (*J. regia*) divided into two genetic sub-clusters: one major cluster contained samples from all over China, and an additional (yellow) cluster dominated by samples from Northwestern China (Xinjiang province, Fig. 3b). At $K = 2$, iron walnut (*J. sigillata*) samples were joined with *J. regia*, but at $K > 2$ they became a coherent genetic group with signs of admixture with *J. regia* (Fig. 3a; Fig. S3). The phylogeny shows iron walnut (*J. sigillata*) samples appear completely embedded within common walnut (*J. regia*) (Fig. S4). When samples within sect. *Dioscaryon* were analyzed separately, they differentiated into $K = 2$ genetic clusters (Fig. 4a). Common walnut (*J. regia*) and iron walnut *J. sigillata* samples divided into distinct groups, with some individuals of mixed ancestry, probably largely from gene introgression (Fig. 4a). *J. sigillata* emerges as a distinct lineage within J. regia in an ML tree based on ~100,000 nuclear SNPs (Fig. 4c). The *PCoA* separated the two *Dioscaryon* species, although *J. sigillata* and *J. regia* exhibited considerable overlap (Fig. 3c). The three major PCs from the *PCoA* explained 18.58% (8.53%, 6.26% and 3.79%, respectively) of the total variance.

Samples of the endangered Ma walnut (*J. hopeiensis*) did not form a coherent genetic cluster at any $K < 5$ and all remained a nearly 50%/50% admixture between (*Dioscaryon* and *Cardiocaryon*) (Fig. S3). At $K = 5$, *J. hopeiensis* samples appeared to be *J. cathayensis/J. mandshurica* × *J. regia* hybrids. FRAPPE analysis of the *J. regia*, *J. hopeiensis*, and *J. mandshurica* (n = 4) samples (excluding *J. sigillata* and *J. cathayensis*) revealed an optimal ΔK for $K = 2$ genetic clusters (Fig. 4d). When the same three species were analyzed at $K = 3$, a second population of *J. regia* emerged and *J. hopeiensis* remained admixed; strongly indicating that *J. hopeiensis* is a hybrid species (Fig. 4b, d). The results of *PCoA* confirm the result from FRAPPE; the cloud of points representing *J. hopeiensis* is midway between *J. mandshurica* and *J. regia* in the space delimited by the three largest PCs (Fig. 3c). In fact, every analytical approach supported the hybrid origin of *J. hopeiensis* (Fig. 3; Fig. 4c,d; Fig. S3, S4).

Phylogenies based on Maximum Likelihood (ML) were strongly similar (Fig. S4). In those trees, *J. cathayensis* and *J. mandshurica* are intermixed, and *J. hopeiensis* appears as intermediate between *J. regia* and the other members of sect. *Cardiocaryon* (Fig. 3d; Fig. S4). *J. hopeiensis*, which is sympatric with *J. mandshurica* (Fig. 3b) constituted two genotypic clusters within section *Cardiocaryon* based on chloroplast data (Fig. S2), but at nuclear SNPs *J. hopeiensis* samples were admixed with roughly equal contributions from species in sect. *Dioscaryon* and *Cardiocaryon* (Figs. 3a, 4c, d, Fig. S4). In phylogenetic trees, *J. hopeiensis* was between the two branches representing *Dioscaryon* and *Cardiocaryon* (Figs. 3d, 4b).

We constructed a phylogenetic tree, based on 45,548 nuclear SNPs by the Bayesian MCMC method (Fig. 5a). To gain an understanding of the time scale of the phylogeny of GBS data, we used 140 indivudals of all five Chinese *Juglans*. The MCMC phylogenetic tree showed that the all samples *Juglans* could be classified into two lineages: lineage I (*J. regia* and *J. sigillata*), lineage II (*J. hopeiensis*, *J. mandshurica*, and *J. cathayensis*). A point estimate for the coalescent time between two sections of *Juglans* was dated to 15.72 Mya, while *J. regia* and *J. sigillata* diverged from 8.85 to 12.39 Mya, and *J. cathayensis* diverged from *J. mandshurica* before 8.86 Mya (Fig. 5a).

3.4. Analysis of molecular variance (AMOVA)

AMOVA based on (45,548) nuclear SNPs revealed a clear species–species separation: $F_{ST} = 0.081$, $P < 0.001$, *J. regia-J. sigillata*; $F_{ST} = 0.118$, $P < 0.001$, *J. sigillata-J. hopeiensis*; $F_{ST} = 0.043$, $P < 0.001$, *J. cathayensis-J. mandshurica*; $F_{ST} = 0.153$, $P < 0.001$, *J. hopeiensis-J. mandshurica*; $F_{ST} = 0.213$, $P < 0.001$, *J. cathayensis -J. hopeiensis*; $F_{ST} = 0.847$, $P < 0.001$, *J. cathayensis-J. regia*; $F_{ST} = 0.296$, $P < 0.001$, *J. hopeiensis-J. regia*, and $F_{ST} = 0.068$, $P < 0.001$, the northern versus southern populations of Chinese *J. regia* (Table S8).

3.5. Phylogenetic analysis using transcriptome data

The average number of genes in each gene family (Table S3), the number of unique gene families (Fig. S5a), and number of genes in unique gene families (Fig. S5b) of the five Chinese walnuts were less than those of *Oryza sativa*, *Glycine* max, and other plants with more complete genomic resources. Nevertheless, 6421 orthologous groups

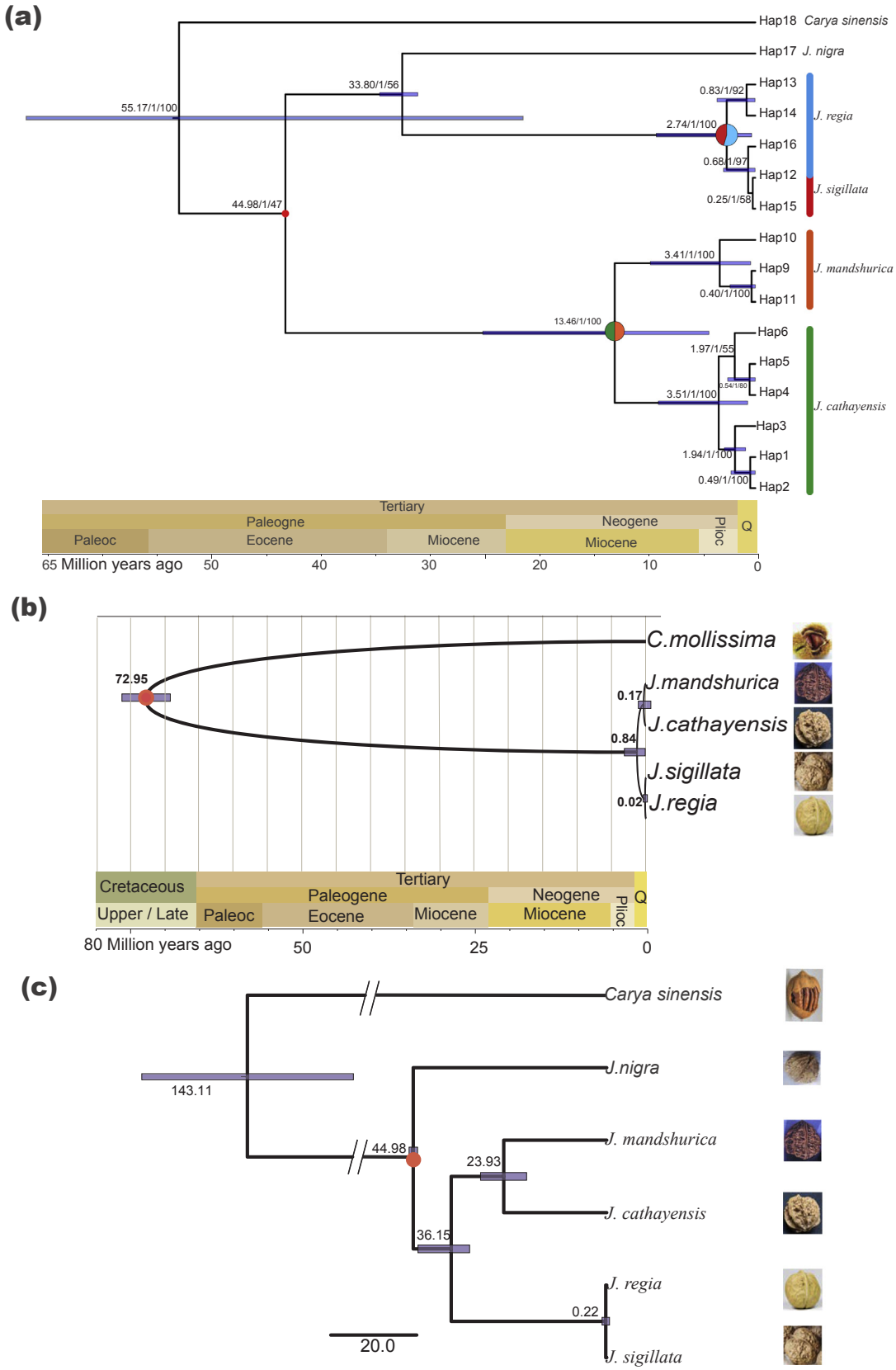

(caption on next page)

were shared by all 14 species used in our analysis (Fig. S5a), which is comparable to previous studies (Fischer et al., 2011). Among the 6421 core orthologous groups, 190 contained only one ortholog in each species (single copy, Fig. S5b).

The alignments of each of the 6421 orthologous genes were separated into four datasets corresponding to each of the three codon

Fig. 2. Phylogenetic tree of Chinese *Juglans* plus *J. nigra*, *Carya sinensis*, and *Castanea mollissima* based on whole chloroplast genome sequences. (a) Phylogenetic timetree of 16 haplotypes plus *J. nigra* and *Carya sinensis* based on whole chloroplast genome sequences. Blue bars and the numbers at nodes indicate 95% highest posterior densities (HPDs) of time estimates (million years ago, Mya). Calibration was based on divergence time estimates of *Juglans* and *Carya* (64.4 ± 0.5 Mya, Manchester and Dilcher, 1997; Zhang et al., 2013). (b) Estimation of divergence time for five Chinese *Juglans* plus *Castanea mollissima* based on whole chloroplast genome sequences. Divergence of *Castanea mollissima* and *Juglans* was estimated at 64.4 ± 0.5 Mya (Manchester and Dilcher, 1997; Zhang et al., 2013). (c) Estimation of divergence time for five Chinese *Juglans* plus *Carya sinensis* based on whole chloroplast genome sequences. Divergence of *J. nigra* and *sect. Cardiocaryon* was estimated at 45 ± 0.5 Mya (Manchester and Garden, 1987; Bai et al., 2016). The geological time scale is in millions of years. Paleoc, Paleocene; Plioc, Pliocene; Q, Quaternary.

positions in the CDS and whole CDS were used to estimate phylogeny. The four datasets resulted in four strongly similar topology structure maximum likelihood trees (Fig. S6). Notably, all the clades leading to *Juglans* species had 100% bootstrap support values (Fig. 3a; Fig. S6). Ma walnut was not included in this phylogenetic analysis because of its apparent origin from recent hybridization. The remaining four taxa separated into two sections (*Dioscaryon* and *Cardiocaryon*) sister to *C. mollissima* (Fagaceae). As shown in Fig. S7a, the divergence between section *Dioscaryon* and section *Cardiocaryon* appears to have occurred ~12.01 million years ago (Mya), during the middle Miocene (based on protein coding sequences) (Fig. 5a), although the timing of their divergence differed considerably if the analysis was based on different codon positions [6.91 Mya, 13.67 Mya, and 33.47 Mya using the first (a), second (b), and third (c) codon positions, respectively (Fig. S7)].

3.6. Ecological niche modeling

The MAXENT models had a high predictive power and were highly accurate (AUC = 0.99). For sect. *Cardiocaryon*, the projection of the model over the present bioclimatic conditions showed that *J. mandshurica* has suitable habitats in northeastern China between 33°N and 48°N, while *J. cathayensis* has habitats in southern China between 20°N and 40°N (Fig. 6a, c). Habitats of *J. mandshurica* and *J. cathayensis* overlapped between 33°N and 40°N (Fig. 1a). *J. hopeiensis* is narrowly distributed in northern China in the hilly, mid-elevation area near Beijing and Tianjin, including parts of Hebei province (Lu et al., 1999; Hu et al. 2015), and it is sympatric with *J. mandshurica*, which may explain why most *J. hopeiensis* contain *J. mandshurica* chloroplast types. For sect. *Dioscaryon*, the ecological niche model (ENM) showed habitat suitability for *J. regia* is between 80°E and 140°E latitude and between 20°N and 44°N longitude. *J. sigillata* is sympatric with *J. regia* and distributed in southern China in Yunnan, Sichuan, Tibet, and Guizhou provinces (Fig. 6d, e).

The reconstructed historical distributions based on climate showed that the predicted range of *J. mandshurica* contracted considerably from the LIG to LGM under the influence of cooler, drier climate, while the predicted range of *J. cathayensis* shifted southeast (Fig. 6a, c). *J. hopeiensis* was predicted to have changed little from the LGM to the present, and at all times was sympatric with *J. mandshurica* (Fig. 6b). Although the main distribution of species in northern China shifted south during the LGM (~21, 000 years BP), and some range contraction occurred, the maps predict that *J. hopeiensis* had suitable habitat over most of its current range 21, 000 years BP (Fig. 6).

Based on jacknife test (Ornelas et al. 2016), the five most important ecological factors were: Precipitation of Warmest Quarter = 19.2%, Mean Temperature of Driest Quarter = 14.2%, Precipitation Seasonality (Coefficient of Variation) = 12.5%, Mean Temperature of Coldest Quarter = 9.34%, and Temperature Seasonality (standard deviation *100) = 9.58%. The loadings of the *PCoA* analysis showed that interactions of temperature and precipitation were the most important factors driving the distribution of *Juglans* species. The *PCoA* showed significant ecological divergence between *J. mandshurica/J. hopeiensis* and *J. regia* (Fig. 7a), but considerable overlap between *J. regia* and *J. cathayensis*. *J. regia* is adapted to a surprisingly large range of conditions, but it did not overlap with *J. mandshurica* or *J. hopeiensis*. *J. regia* and *J. sigillata* occupied the same habitats in Southern China and Xinjiang province. *J. hopeiensis* habitats more closely resembled *J. mandshurica* than any other *Juglans* species (Fig. 7a). The degree of ecological niche overlap among *Juglans* species and different lineages (ecological divergence) showed that the ranges of many Chinese *Juglans* overlap (e.g., *J. regia/J. sigillata* and *J. mandshurica/J. cathayensis/J. hopeiensis*), but they may not share niches within the same locations (e.g., *J. regia* and *J. sigillata*; Fig. 7b). The ENMs revealed that *J. regia* is climatically more restricted than other *Juglans* species (Fig. 7b–d; Fig. S8). All species of *Juglans* occupy a smaller range than the area predicted to be climatically suitable. Because we trained ENMs on individual species, this type of range over-prediction indicates that the climate variables we examined are not the main factors limiting *Juglans* species' dispersal and gene flow. Inspection of the spatial overlap between ENMs (Fig. 6) revealed that factors other than those described in the ENM maintain parapatry for *J. regia* and *J. mandshurica*, *J. mandshurica* and *J. cathayensis* (Fig. S8), while *J. hopeiensis* is climatically less restricted than other *Juglans* species (Fig. S8).

4. Discussion

Our results provide important insight into the evolution and biogeography of Chinese *Juglans*. Prior studies of Chinese *Juglans* species based on chloroplast sequences and SSRs from many individual trees (Bai et al., 2014, 2016; Wang et al., 2016) or genomic sampling from a few individuals (Wang et al., 2008, 2015; Bai et al., 2016) revealed deep phylogeographic structure associated with major landscape features. Our Cp genome and GBS data is consistent with the same phylogeographic breaks, but we also found that post-Quaternary dispersal of *J. regia* and its interaction with other species and formerly distinct *J. regia* lineages led to the human propagation of novel taxa.

4.1. The status of Juglans hopeiensis

Genomic data from GBS and orthologous sequences analyzed using ML, BI, NJ, and FRAPPE strongly indicated that *J. hopeiensis* is a hybrid (*J. mandshurica* × *J. regia*) or (*J. cathayensis* × *J. regia*) species (Figs. 1, 3, Figs. S3, S4), most likely maintained as such by human selection for nut phenotypes valued in commercial trade. A similar conclusion was suggested based on randomly amplified polymorphic DNA (RAPD) markers, isozyme, and karyotype analysis (Rehder, 1940; Wu et al., 1999; Mu et al., 1990), although *J. mandshurica* was generally considered the female parent and *J. regia* the male (Wu et al., 1999; Mu et al., 1990) a conclusion contradicted by our genomic analysis of chloroplasts (Fig. 1). The presence of *J. cathayensis* × *J. regia* hybrids among *J. hopeiensis* samples was unexpected and to our knowledge has not been previously reported. The origin of *J. hopeiensis* as an intersectional hybrid probably explains its low fertility (Dai et al., 2014). It is not surprising that *J. hopeiensis* occupies sites that are bioclimatically distinct from *J. regia* and *J. mandshurica* (Fig. S8) because other *Juglans* hybrids have been shown to do so (Crystal et al., 2016). The presence of a private chloroplast haplotype within *J. hopeiensis* derived from both *J. cathayensis* and *J. mandshurica* may indicate that distinct lineages of these species were found in the area now occupied by *J. hopeiensis*. These lineages may have been isolated from other conspecifics during glaciations and subject to gene flow from *J. regia* after that species was introduced to northern China by human dispersal (Pollegioni et al.,

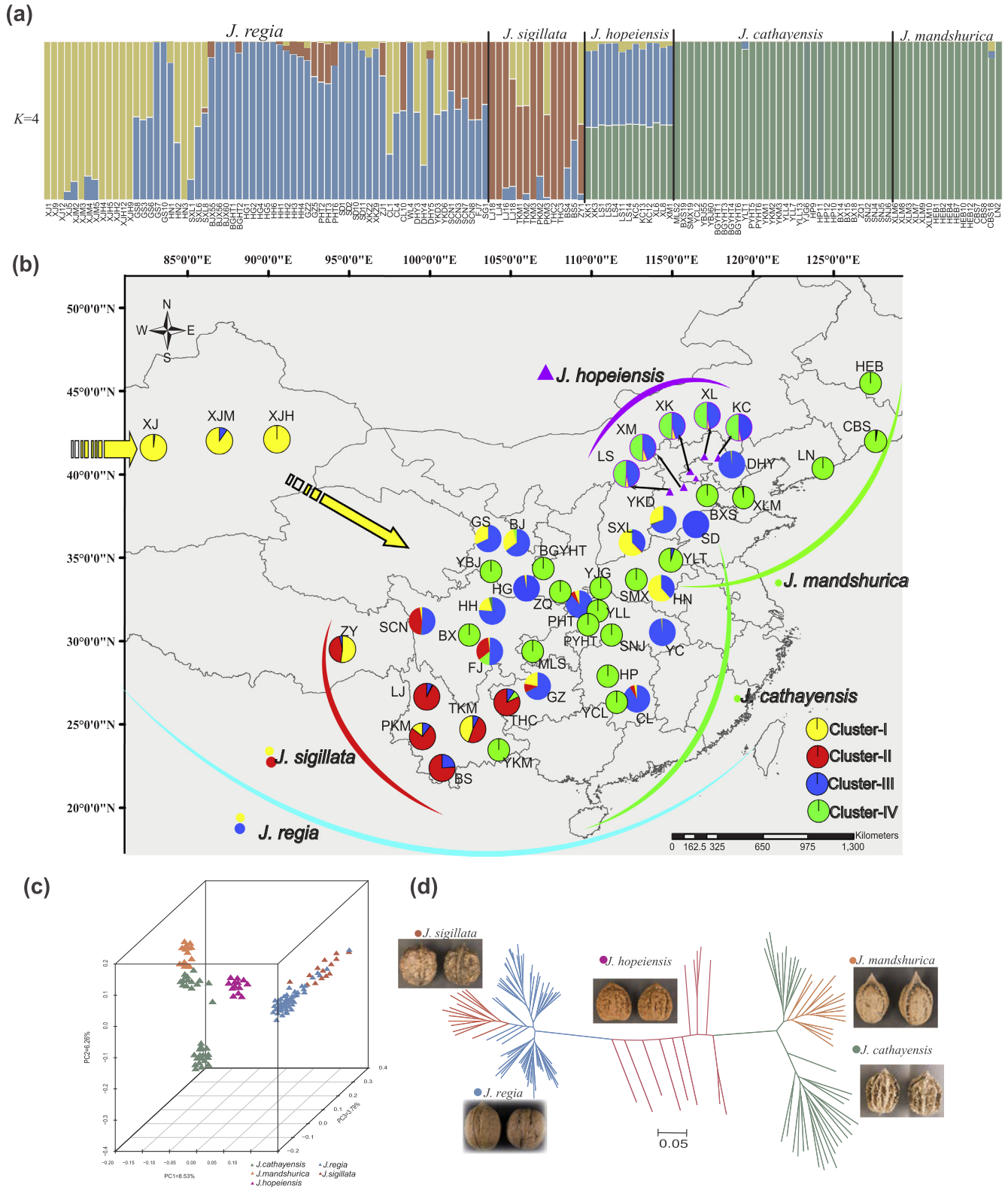

Fig. 3. Geographical distribution and population structure of Chinese *Juglans*. (a) Population structure analysis of genotypes of five Chinese *Juglans* at (the predicted optimal) $K = 4$ based on FRAPPE software; samples included 140 individuals from 47 locations (Table 1). Analyses were based on 45,548 SNPs with 20 iterations for each K for 500,000 iterations. Each individual is represented by a vertical bar. The most likely number of genetic clusters (optimal $K = 4$) was determined using ADMIXTURE (Alexander et al., 2009) (b) Geographical distribution of sample sites of five Chinese *Juglans*; colors of four clusters correspond of those in the legend in the right corner of the map, for each population, percent membership in each of the four genetic clusters is indicated with a pie chart. (c) Principal coordinate analyses (*PCoA*) based on GBS SNPs. (d) Maximum Likelihood (ML) tree (unrooted) based on nuclear SNPs. Colored branches represent the non-admixed individuals within each corresponding group, colors are as indicated in (c). All major nodes have 100% bootstrap support.

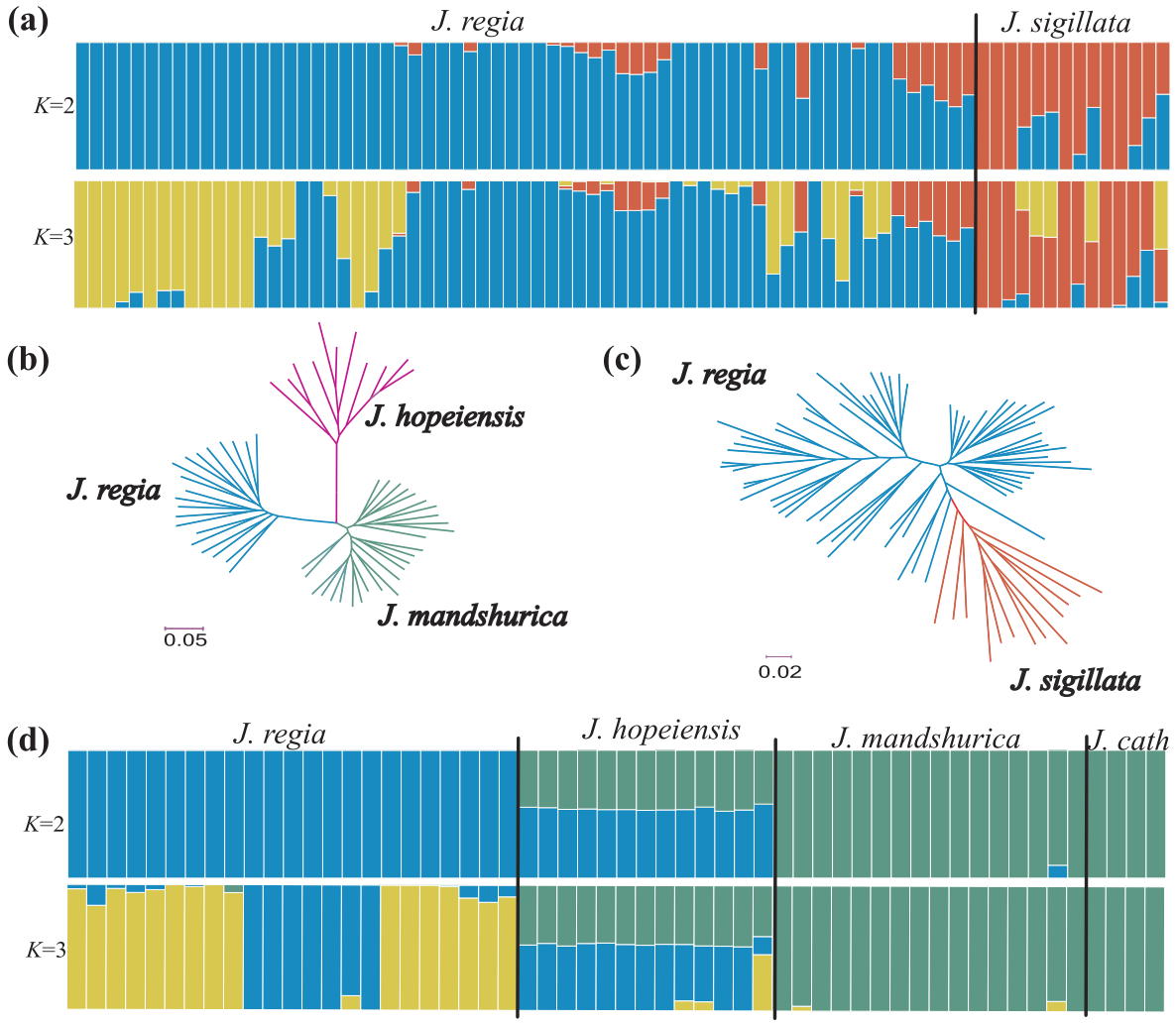

Fig. 4. Population structure analysis of Chinese *Juglans*. Probability of membership in each of the Q-plots was based on Bayesian model-based clustering of 45,548 SNPs obtained using GBS. (a) Genetic structure analysis of *J. regia* and *J. sigillata* from $K = 2$ to 3. Shown is the histogram for the most likely K value (two populations) as indicated by Delta K (Evanno et al., 2005). (b) Maximum Likelihood (ML) tree of *J. regia*, *J. hopeiensis*, and *J. sigillata* based on 54,939 nuclear SNPs. (c) Maximum Likelihood (ML) tree of samples of *J. regia*, and *J. sigillata* based on 103,574 nuclear SNPs. (d) Genetic structure analysis of *J. regia*, *J. hopeiensis*, *J. cathayensis*, and *J. mandshurica* from $K = 2$ to 3 (the better K value was 2). (e) Genetic structure analysis of *J. cathayensis* and *J. mandshurica* from $K = 2$ to 3 (the better K value was 2).

2015). Our data show the chloroplast haplotypes in *J. hopeiensis* were derived from existing haplotypes H9 (*J. mandshurica*) about 1 Mya, and H7 (*J. cathayensis*) about 1.3 Mya (Fig. S2). The recent derivation of *J. hopeiensis* (timed with the arrival of *J. regia* and subsequent hybridization of *J. regia* with local sect. *Cardiocaryon* species), and its derivation from both *Cardiocaryon* species argue that *J. hopeiensis* should be considered a horticultural variety, rather than a species. *J. hopeiensis* does not occupy an ecological niche that strongly separates it from other *Juglans* species, which could potentially explain the gene flow between geographically adjacent populations of the two sections (Fig. S8). Future studies assessing the fine-scale ecological characteristics of *Juglans* species in relation to genetic patterns could clarify the role of environmental factors in limiting gene flow among populations in different sections of *Juglans*.

4.2. The status of Juglans sigillata

Our data provide strong evidence that *J. sigillata* is a sub-species or, perhaps, a landrace of *J. regia*. *Juglans sigillata* was first proposed as a species by Dode (1906), who distinguished it from *J. regia* (as well as *J. fallax*, *J. orientalis*, and *J. sinensis* which Rehder later identified as *J. mandshurica* × *J. regia*, a generally accepted conclusion) primarily based on characteristics of the nut. Of all the members of sect. *Dioscaryon* described in detail by Dode, only *J. regia* and *J. sigillata* remain widely accepted (Flora of China, 1999). Whether *J. sigillata* is distinct from *J. regia*, or an ecotype has been controversial. Manning (1978) lumped them together based on morphology, Grimshaw (2003) did not. Gunn et al. (2010) concluded that the species were morphologically distinct, but not separable based on 14 microsatellites. Wang et al., 2015 agreed the species are morphologically distinct, but also found about 8% of total variance at 12 SSR loci was between species, and based on Bayesian analysis of genetic structure concluded the species were genetically distinct as well. Our data showed that *J. sigillata* contained at least one chloroplast haplotype not shared by *J. regia* (H15, Table 1), but that this haplotype was derived from a *J. regia* haplotype (Fig. 1; Fig. S1) and its estimated divergence time from *J. regia* was only 0.25 Mya/0.02 Mya/0.22 Mya (Fig. 2). Unlike Wang et al. (2015), our genetic structure analysis was based on (45,548) SNPs, but like Wang et al. (2015), we found that the two species were clearly separated with some admixture (Figs. 3, 4a,b, Fig. S3 at all $K \geq 3$). Structure analysis is not designed to identify species, however, but differences among populations. A maximum likelihood phylogeny based on 45,548 SNPs

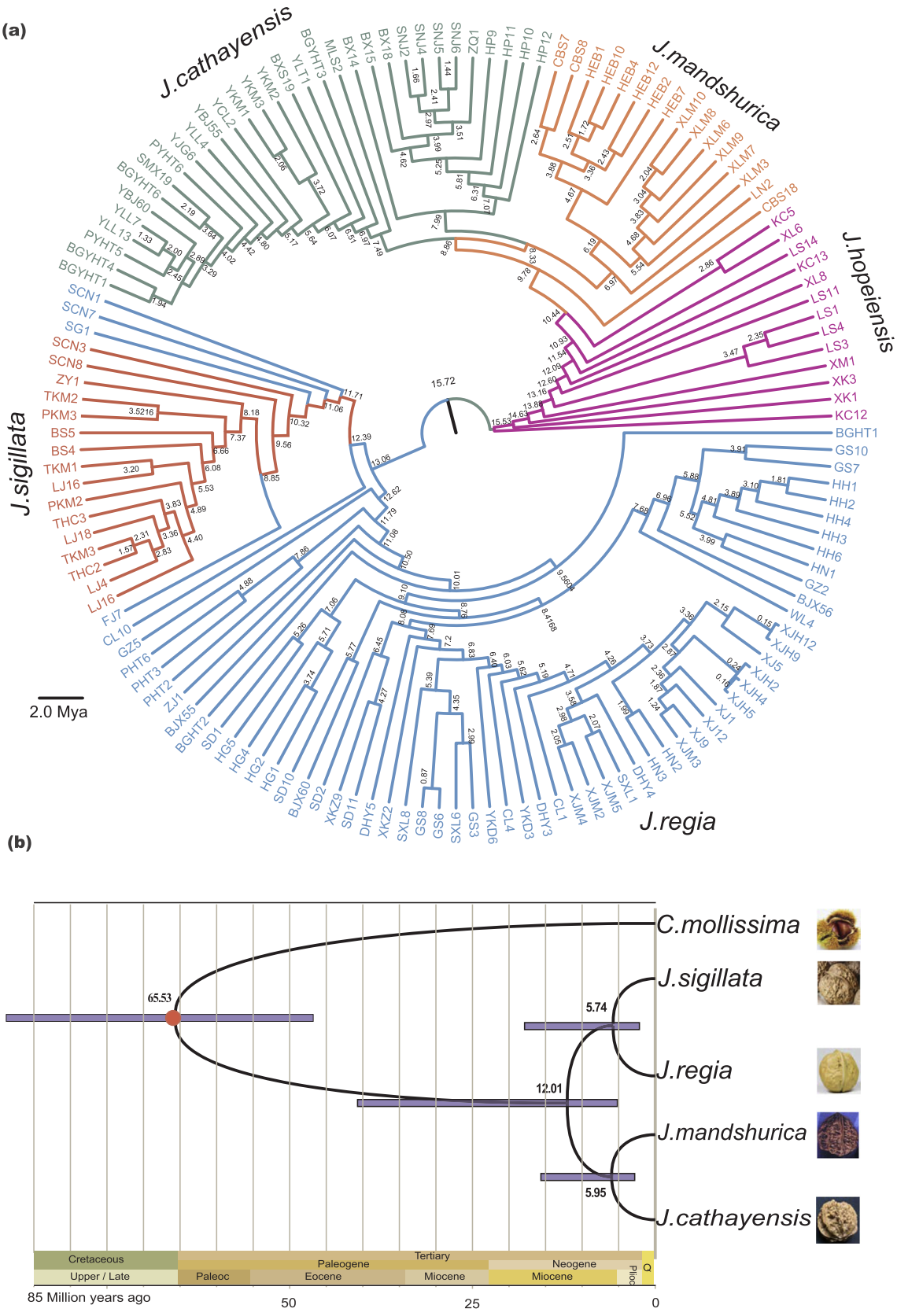

Fig. 5. Phylogenetic timetrees of Chinese *Juglans* based on genotype by sequencing (GBS) data and transcriptome CDS (protein coding sequences). (a) Phylogenetic timetree of 140 *Juglans* individuals based on 45,548 SNPs constructed using the Bayesian MCMC method. Divergence of *sect. Dioscaryon* and *sect. Cardiocaryon* was estimated at 15 ± 5 Mya (Manchester and Garden, 1987; Bai et al., 2016). Divergence times (Mya) are shown at each node. (b) Phylogenetic timetree based on CDS. The purple bars at the nodes indicate 95% posterior probability intervals. Divergence of *Castanea mollissima* and *Juglans* was estimated at 64.4 ± 0.5 Mya (Manchester and Dilcher, 1997; Zhang et al., 2013). The geological time scale is in millions of years. Paleoc, Paleocene; Plioc, Pliocene; Q, Quaternary.

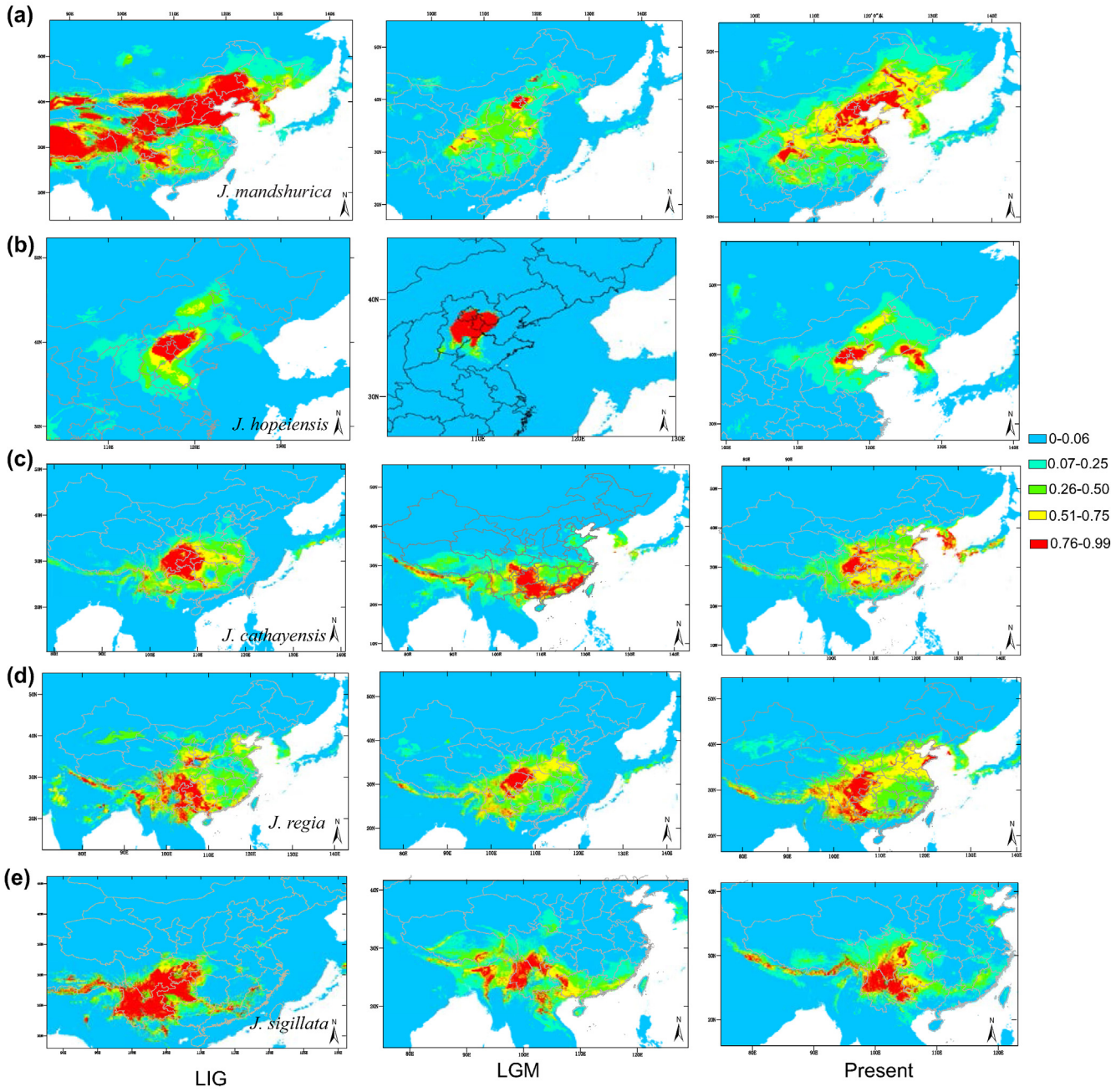

Fig. 6. Ecological niche models of *Juglans mandshurica* (a), *J. hopeiensis* (b), *J. cathayensis* (c), *J. regia* (d), and *J. sigillata* (e). Average projections of the model to the last glacial maximum [circa 21 kyr before present (BP)] using the Model for Interdisciplinary Research on Climate (MIROC) general circulation model simulations for each of the five Chinese *Juglans*. LIG = Average projection of the model to the last interglacial (120–140 kyr BP). Present = predicted distribution probability (as a logistic value) for current climatic conditions for all five Chinese *Juglans* species.

(Figs. 3d, 4c) showed all *J. sigillata* samples were embedded within *J. regia*. The same result was obtained using ML based on whole genome data (Fig. S4). Divergence time estimates based on protein coding sequences and GBS SNPs showed *J. sigillata* and *J. regia* separated about the same time as *J. mandshurica* and *J. cathayensis* (Fig. 5a, b; Table S10), but in sect. *Dioscaryon* the chloroplast data show *J. sigillata* to be a genetic subset of *J. regia*. We found no clear evidence that *J. sigillata* was a lineage independent of *J. regia*. *Juglans sigillata* appears to be maintained as a distinct landrace, possibly by ecological isolation (Wang et al., 2015), although we found that the bioclimatic envelopes of the taxa overlap (Figs. 6, 7a). It is more likely *J. sigillata* is kept distinct from *J. regia* by human selection (Gunn et al., 2010).

4.3. *Juglans regia* in China

In common walnut (*J. regia*), the SNP-based phylogeny and analysis of genetic structure showed two subpopulations in China, with a clear geographic genetic break corresponding to divergence between the Xinjiang Province and other regions (Figs. 3, 4; Pollegioni et al., 2015). This north/south divide in *J. regia* may reflect a broader divide in east Asian phylogeography (Bai et al., 2016), the general genetic structure of *J. regia* in Asia (Pollegioni et al., 2014), or distinct introductions of *J. regia* into China. Although the origin of *J. regia* is obscure (Martínez-García et al., 2016), historical biogeography and presumed locations of Quaternary glacial refugia led Aradhya et al. (2007) to suggest the species had multiple centers of origin. None of the proposed refugia are

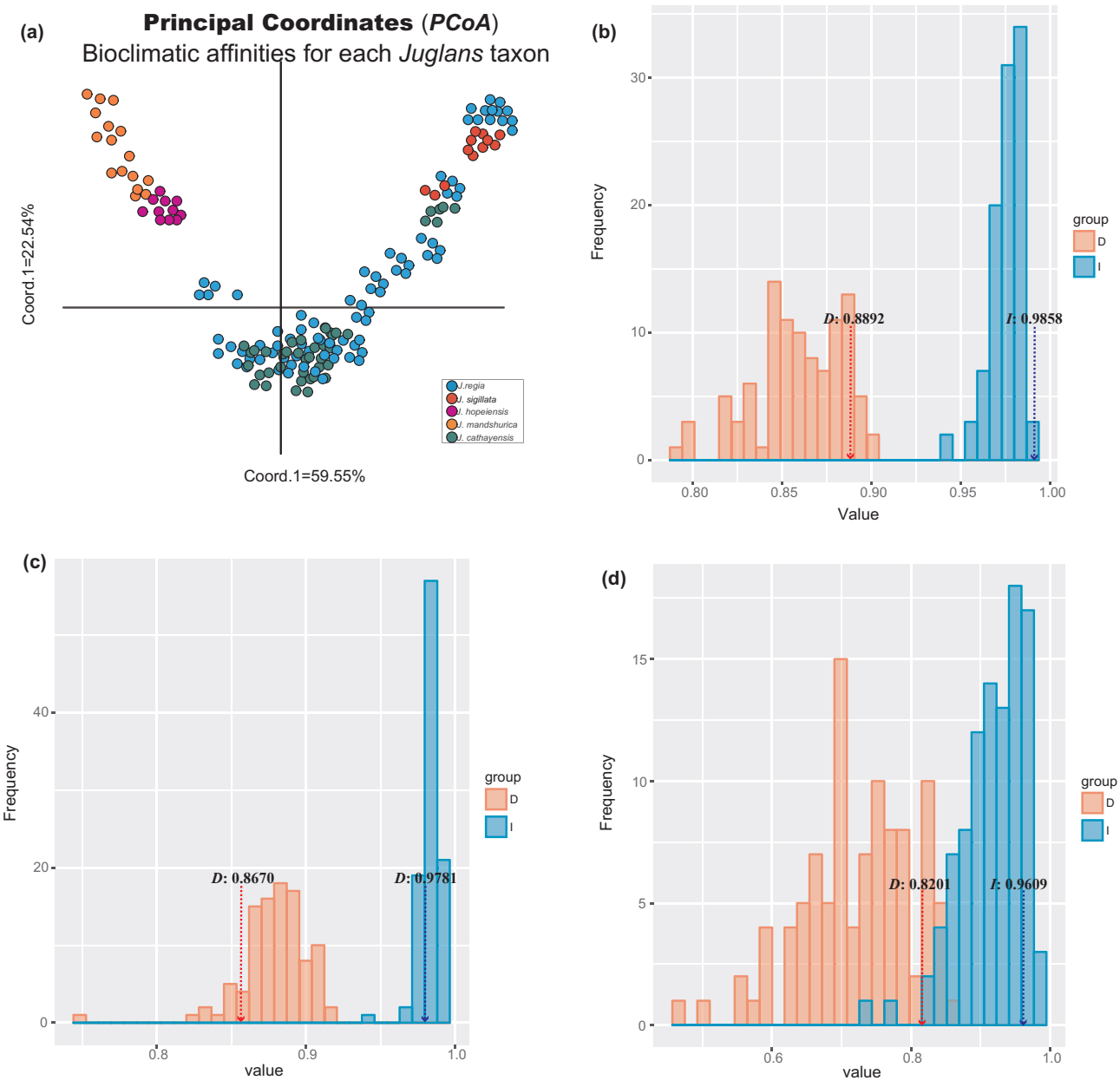

Fig. 7. Plot of sampled sites or occurrence data for each of five Chinese *Juglans* onto two principal components that summarize 82.1% of variance in 19 bioclimatic layers. Each taxon is represented by a different color, as indicated in the box at lower right of (a); (b) Niche identity tests for *J. regia/J. sigillata*, (c) Niche identity test for *J. regia/J. mandshurica*, and (d) Niche identity test of sub-cluster I of *J. regia/* sub-cluster II of *J. regia.* Phylogeographic groups based on 6 bioclimatic variables (Bio3, Bio4, Bio9, Bio11, Bio15, and Bio18). Light red indicates Schoener's *D* and its null distributions of 100 pseudoreplicates; Light blue indicates Warren et al.,'s *I* and its null distributions of 100 pseudoreplicates. The dashed lines denote the observed values of Schoener's *D* (0.889) and Hellinger's *I* (0.986) with significant *P* values for both niche overlap measures ($P < 0.001$). For additional analyses of niche overlap among *Juglans* species and different lineages, see Fig. S8.

in central or southern China, however, but instead in Tibet and possibly Xinjiang, so the genetic structure of *J. regia* in China has probably been determined by (relatively recent) human selection and dispersal (Pollegioni et al., 2015). Common walnuts from far-western China (Xinjiang province) were likely the ancestors of populations distributed in central and northern China (Fig. 1; 3b), and *J. regia* from southern China (especially in Yunnan province) may represent a separate source population for *J. regia* in China (Fig. 1, Fig. S4; Pollegioni et al., 2015). Confirming the origins and history of *J. regia* in Asia represents an important goal, especially for regions where cultivation and selection or isolation and adaptation may have been potent drivers of genetic change. Research of this type is a particular challenge without a publicly available, high-quality genome assembly. Once such a resource is developed, the loci underlying population divergence between closely relative species and within species can be identified (Schlötterer et al., 2014).

4.4. *Juglans cathayensis and mandshurica*

J. mandshurica and *J. cathayensis* are considered the two Chinese members of sect. *Cardiocaryon*, but some have lumped them into a single species (Lu et al., 1999; Grimshaw, 2003) along with *J. collapsa* Dode, *J. draconis* Dode, and *J. stenocarpa* Maxim. The independence of *J. mandshurica* and *J. cathayensis* has been asserted historically ('Ye Hu tao', *J. cathayensis* versus 'Hu tao qiu', *J. mandshurica*), in classical taxonomy (Dode, 1909, although Dode was without doubt an unreformed taxonomic "splitter"), and in recent molecular analyses (Aradhya et al., 2007). Our samples of *J. cathayensis* contained a total of

six chloroplast haplotypes, and each of the six sampled populations was fixed for a single haplotype, displaying the pronounced phylogeographic structure previously remarked upon by Bai et al. (2016) (Fig. 1, Table 1). Bai et al. (2016) identified nine haplotypes in *J. cathayensis*, all distinct from those of *J. mandshurica*. These results, and ecological niche models, are evidence that *J. cathayensis* populations survived the last glaciation *in situ*, although they were probably more fragmented than today (Fig. 6c; Fig. S8; Bai et al., 2014). The timing of the divergence of the chloroplast lineages common to all *J. cathayensis* from those of *J. mandshurica* was probably the late Miocene (Bai et al., 2016), which was confirmed by our analysis [13.45 Mya (Fig. 2a)], but this reconstruction depended heavily on the fossil calibration (0.17 Mya in Fig. 2b and 22.93 Mya in Fig. 2c), a conclusion shared by Bai et al. (2016).

The genetic structure of *Cardiocaryon* in China at nuclear loci (based on GBS data) indicated *J. cathayensis* and *J. mandshurica* were separated at the optimal $K = 2$. Samples from populations HP, BX and SNJ from Hunan, Sichuan, and Hubei, showed subtle admixture with *J. mandshurica* when the analysis was expanded to include sect. *Dioscaryon* samples (at $K = 5$ and $K = 8$; Fig. S3), The ML trees (Fig. 3d, Fig. S4), and *PCoA* (Fig. 3c) also showed samples of *J. cathayensis* from the same populations (BX, HP, and SNJ) clustered with *J. mandshurica*. Bai et al. (2014, 2016) found evidence of weak genetic structure within the nuclear genome of *J. cathayensis*, but it was associated with admixture with *J. mandshurica* in northern populations, not with samples of BX, HP, or SNJ that were sampled by Bai et al. (2016). They reported an *F*ST of 0.11 among *J. cathayensis*, considerably higher than our estimate of 0.043 between *J. cathayensis* and *J. mandshurica*, although we sampled fewer and less dispersed populations. In any case, nuclear gene flow among *J. cathayensis* populations is probably sufficient to keep them "well-connected" (Bai et al., 2014), so we have no explanation for the subtle structure we observed in our *J. cathayensis* samples.

Manchurian walnut (*J. mandshurica*) is distributed parapatrically with *J. cathayensis*; their predicted habitats potentially overlap based on our bioclimate models (Fig. 5), but in fact they are adapted to distinct climates [Fig. 6, Fig. S8; see also Bai et al. (2016)]. *J. mandshurica* is allopatric with *J. ailantifolia*, its closest relative, which is native to Japan. The three Asian butternuts (sect. *Cardiocaryon*) are closely related, with small morphological differences (Grimshaw, 2003): *J. mandshurica* has often been characterized as a species with abaxially glabrescent leaflets and a fruiting spike with four or five nuts, whereas *J. cathayensis* is described as having tomentose leaflets and a flowering spike that typically bears six to ten nuts (Lu et al., 1999; Bai et al., 2016); *J. cathayensis* nuts were described as larger than those of *J. mandshurica*, with a more acute apex and a less sharp external roughness (Dode, 1909). The split between the closely related species *J. cathayensis* and *J. mandshurica* occurred 0.17 to 23.93 Mya based on chloroplast genomes; the most recent estimate is derived when *C. mollissima* as the outgroup, the oldest estimate is derived when *C. sinensis* is used (Table S10). The analysis of their divergence time based on nuclear data is nearly as inconclusive; an estimate of 2.0–26.05 Mya is obtained when CDS (orthologous genes), first, second, or third codon positions are analyzed (Table S10). Where *J. mandshurica* and *J. cathayensis* are placed in the continuum between ecological races or varieties and species is not obvious from the data (Mallet, 2008). The observation that the two taxa can hybridize and produce fertile progeny is probably irrelevant, as intersectional (and intercontinental) hybrids are often fertile in *Juglans* (Pollegioni et al., 2009).

We identified three chloroplast haplotypes within *J. mandshurica*, and perhaps an additional *J. mandshurica* haplotype private to *J. hopeiensis* (Fig. 1). This diversity was significant because Bai et al. (2016) considered the northern (i.e., Chinese) populations of *J. mandshurica* to have undifferentiated chloroplasts and therefore postulated a single refugium for them. It is certainly possible that *J. mandshurica* had multiple and isolated Chinese refugia (similar to *J. cathayensis*) but that all were separated from those of *J. cathayensis* after the species diverged in the late Miocene (Fig. S2, Bai et al., 2016), maintaining the phylogeographic break suggested in Bai et al. (2016). We did not observe any evidence of genetic substructure at nuclear loci within *J. mandshurica* based on our limited samples, although Bai et al. (2016) suggested a break between two populations at about 125 °E longitude that is different than the Korean versus Chinese *J. mandshurica* genetic pools indicated in chloroplast phylogeny.

The evidence indicates sect. *Cardiocaryon* divided into *J. mandshurica* (northern China) and *J. cathayensis* (southern China) during the Neogene, possibly as late as the Pliocene. Gene introgression by pollen flow kept the species connected. In sect. *Dioscaryon*, *J. regia* and *J. sigillata* divided more recently than the split in sect. *Cardiocaryon* (Figs. 2, 5, Fig. S7), and it appears human management of both taxa in the section will determine whether *J. sigillata* remains distinct (Gunn et al. 2010). Notwithstanding the presence of *J. hopeiensis*, which is probably only viable as a horticultural variety, we found no evidence for substantial gene flow between sect. *Cardiocaryon* and sect. *Dioscaryon* in natural populations (Figs. 1, 3; Fig. 7a; Fig. S8), although their distributions overlap in China.

Acknowledgments

This work was supported by the National Natural Science Foundation of China (No. 41471038, 31200500, and J1210063), Changjiang Scholars and Innovative Research Team in University (No. IRT1174), and the Program for Excellent Young Academic Backbones Funding by Northwest University (No. 338050070). Mention of a trademark, proprietary product, or vendor does not constitute a guarantee or warranty of the product by the U.S. Department of Agriculture and does not imply its approval to the exclusion of other products or vendors that also may be suitable.

Data accessibility

The sequences reported in this paper were deposited in the National Center for Biotechnology Information (NCBI) Sequence Read Archive (SRA) and Transcriptome Shotgun Assembly (TSA). Raw paired-end reads are available through the NCBI SRA under accession numbers: SRX1295882, SRX1734262. The complete Cp genome of all five *Juglans* species were deposited in NCBI GenBank (Hu et al., 2016, 2017; accession numbers, KT963008, KX671976, KX671977, KX671975, and KT963008).

Appendix A. Supplementary material

Supplementary data associated with this article can be found, in the online version, at https://doi.org/10.1016/j.ympev.2018.04.014.

References

Alexander, D.H., Novembre, J., Lange, K., 2009. Fast model-based estimation of ancestry in unrelated individuals. Genome Res. 19, 1655–1664.
Aradhya, M.K., Potter, D., Gao, F., Simon, C.J., 2007. Molecular phylogeny of *Juglans* (Juglandaceae), a biogeographic perspective. Tree Genet. Genomes 3, 363–378.
Bai, W.N., Wang, W.T., Zhang, D.Y., 2014. Contrasts between the phylogeographic patterns of chloroplast and nuclear DNA highlight a role for pollen-mediated gene flow in preventing population divergence in an East Asian temperate tree. Mol. Phylogenet. Evol. 81, 37–48.
Bai, W.N., Wang, W.T., Zhang, D.Y., 2016. Phylogeographic breaks within Asian butternuts indicate the existence of a phytogeographic divide in East Asia. New Phytol. 209, 1757–1772.
Bankevich, A., Nurk, S., Antipov, D., Gurevich, A.A., Dvorkin, M., Kulikov, A.S., Lesin, V.M., Nikolenko, S.I., Pham, S., Prjibelski, A.D., et al., 2012. SPAdes, a new genome assembly algorithm and its applications to single-cell sequencing. J. Comput. Biol. 19, 455–477.
Chevreux, B., Pfisterer, T., Drescher, B., Driesel, A.J., Müller, W.E.G., Wetter, T., Suhai, S., 2004. Using the miraEST assembler for reliable and automated mRNA transcript assembly and SNP detection in sequenced ESTs. Genome Res. 14, 1147–1159.
Collins, W.D., Rasch, P.J., Boville, B.A., Hack, J.J., McCaa, J.R., Williamson, D.L., Briegleb, B.P., Bitz, C.M., Lin, S.J., Zhang, M., 2006. The formulation and atmospheric simulation of the Community Atmosphere Model version 3 (CAM3). J. Climate 19, 2144–2161.
Crystal, P.A., Lichti, N.I., Woeste, K.E., Jacobs, D.F., 2016. Vegetative and adaptive traits

predict different outcomes for restoration using hybrids. Front. Plant Sci. 7, 1741.
Dai, S.J., Qi, J.X., Duan, C.R., Wang, Y.P., Chen, P., Li, Q., Hao, Y.B., Leng, P., 2014. Abnormal development of pollen and embryo sacs contributes to poor fruit set in walnut (*Juglans hopeiensis*). J. Hortic. Sci. Biotech. 89, 273–278.
Dang, M., Liu, Z., Chen, X., Zhang, T., Zhou, H., Hu, Y., Zhao, P., 2015. Identification, development, and application of 12 polymorphic EST-SSR markers for an endemic Chinese walnut (*Juglans cathayensis* L.) using next-generation sequencing technology. Biochem. Syst. Ecol. 60, 74–80.
Dang, M., Zhang, T., Hu, Y., Zhou, H., Woeste, K., Zhao, P., 2016. De novo assembly and characterization of bud, leaf and flowers transcriptome from *Juglans regia* L. for the identification and characterization of new EST-SSRs. Forests 7, 247.
Daniell, H., Lin, C.S., Yu, M., Chang, W.J., 2016. Chloroplast genomes, diversity, evolution, and applications in genetic engineering. Genome Biol. 17, 134.
Davey, J.W., Hohenlohe, P.A., Etter, P.D., Boone, J.Q., Catchen, J.M., Blaxter, M.L., 2011. Genome-wide genetic marker discovery and genotyping using next-generation sequencing. Nat. Rev. Genet. 12, 499–510.
Dode, L.A., 1906. Contribution a l'étude du genre *Juglans*. Bulletin de la Societé Dendrologique de France, 2, 67–97.
Dode, L.A., 1909. Contribution a l'étude du genre *Juglans*. Bulletin de la Societé Dendrologique de France, 11, 22 – 50.
Dodsworth, S., Chase, M.W., Kelly, L.J., Leitch, I.J., Macas, J., Novák, P., Piednoël, M., Weiss-Schneeweiss, H., Leitch, A.R., 2015. Genomic repeat abundances contain phylogenetic signal. Syst. Biol. 64, 112–126.
Dowell, S.A., Hekkala, E.R., 2016. Divergent lineages and conserved niches, using ecological niche modeling to examine the evolutionary patterns of the Nile monitor (*Varanus niloticus*). Evol. Ecol. 30, 471–485.
Draine, B., Hiden, M. 1998. The Walnut Cookbook. Berkeley.
Elshire, R.J., Glaubitz, J.C., Sun, Q., Poland, J.A., Kawamoto, K., Buckler, E.S., Mitchell, S.E., 2011. A robust, simple genotyping-by-sequencing (GBS) approach for high diversity species. PLoS One 6, e19379.
Escudero, M., Eaton, D.A., Hahn, M., Hipp, A.L., 2014. Genotyping-by-sequencing as a tool to infer phylogeny and ancestral hybridization, A case study in *Carex* (Cyperaceae). Mol. Phylogenet. Evol. 79, 359–367.
Evanno, G., Regnaut, S., Goudet, J., 2005. Detecting the number of clusters of individuals using the software STRUCTURE: a simulation study. Mol. Ecol. 14, 2611–2620.
Fischer, S., Brunk, B.P., Chen, F., Gao, X., Harb, O.S., Iodice, J.B., Shanmugam, D., Roos, D.S., Stoeckert, C.J., 2011. Using OrthoMCL to assign proteins to orthoMCL-DB groups or to cluster proteomes into new ortholog groups. Curr. Protocols Bioinformatics 35, 11–16.
Fjellstrom, R.G., Parfitt, D.E., 1995. Phylogenetic analysis and evolution of the genus *Juglans* (Juglandaceae) as determined from nuclear genome RFLPs. Plant Syst. Evol. 197, 19–32.
Forster, P., Ro, A., 1994. Median-Joining networks for inferring intraspecific phylogenies. Mol. Biol. Evol. 16, 37–48.
Gunn, B.F., Aradhya, M., Salick, J.M., Miller, A.J., Yongping, Y., Lin, L., Xian, H., 2010. Genetic variation in walnuts (*Juglans regia* and *J. sigillata*; Juglandaceae), species distinctions, human impacts, and the conservation of agrobiodiversity in Yunnan. China. Am. J. Bot. 97, 660–671.
Grimshaw, J., 2003. IDS Yearbook: Notes on the temperate species of *Juglans*, pp. 107–130.
Hahn, C., Bachmann, L., Chevreux, B., 2013. Reconstructing mitochondrial genomes directly from genomic next-generation sequencing reads—a baiting and iterative mapping approach. Nucleic Acids Res. 41, e129.
Hu, Y.H., Zhao, P., Zhang, Q., Wang, Y., Gao, X.X., Zhang, T., Zhou, H.J., Dang, M., Woeste, K.E., 2015. De novo assembly and characterization of transcriptome using Illumina sequencing and development of twenty five microsatellite markers for an endemic tree *Juglans hopeiensis* Hu in China. Biochem. Systemat. Ecol. 63, 201–211.
Hu, Y., Woeste, K.E., Dang, M., Zhou, T., Feng, X., Zhao, G., Liu, Z., Li, Z., Zhao, P., 2016. The complete chloroplast genome of common walnut (*Juglans regia*). Mitochondrial DNA Part B 1, 189–190.
Hu, Y.H., Woeste, K.E., Zhao, P., 2017. Completion of the chloroplast genomes of five Chinese *Juglans* and their contribution to chloroplast phylogeny. Front. Plant Sci. 7, 1955.
Jansen, R.K., Saski, C., Lee, S.B., Hansen, A.K., Daniell, H., 2011. Complete plastid genome sequences of three rosids (*Castanea*, *Prunus*, *Theobroma*), evidence for at least two independent transfers of *rpl22* to the nucleus. Mol. Biol. Evol. 28, 835–847.
Katoh, K., Standley, D.M., 2013. MAFFT multiple sequence alignment software version 7, improvements in performance and usability. Mol. Biol. Evol. 30, 772–780.
Kuang, K.Z., Lu, A.M., 1979. Flora of China. Science Press, Beijing, China.
Langmead, B., Salzberg, S.L., 2012. Fast gapped-read alignment with Bowtie 2. Nat. Methods 9, 357–359.
Li, H., Coghlan, A., Ruan, J., Coin, L.J., Hériché, J.K., Osmotherly, L., Li, R., Liu, T., Zhang, Z., Bolund, L., et al., 2006. TreeFam, A curated database of phylogenetic trees of animal gene families. Nucleic Acids Res. 34, D572–D580.
Li, H., Durbin, R., 2009. Fast and accurate short read alignment with Burrows-Wheeler transform. Bioinformatics 25, 1754–1760.
Li, H., Handsaker, B., Wysoker, A., Fennell, T., Ruan, J., Homer, N., Marth, G., Abecasis, G., Durbin, R., 2009. The sequence alignment/map format and SAMtools. Bioinformatics 25, 2078–2079.
Librado, P., Rozas, J., 2009. DnaSP v5, a software for comprehensive analysis of DNA polymorphism data. Bioinformatics 25, 1451–1452.
Leigh, J.W., Bryant, D. 2015. popart, full-feature software for haplotype network construction (S Nakagawa, Ed,). Methods Ecol. Evol. 6, 110–1116.
Lipka, A.E., Tian, F., Wang, Q., Peiffer, J., Li, M., Bradbury, P.J., Gore, M.A., Buckler, E.S., Zhang, Z., 2012. GAPIT, genome association and prediction integrated tool. Bioinformatics 28, 2397–2399.
Lu, A.M., Stone, D.E., Grauke, L.J. 1999. Juglandaceae. Flora of China, 4, 277–285. St. Louis, Missouri, Missouri Botanic Garden Press. Online version, http,//www.efloras.org/flora_page.aspx?flora_id = 2.
Mallet, J., 2008. Hybridization, ecological races and the nature of species, empirical evidence for the ease of speciation. Philos. T. R. Soc. B 363, 2971–2986.
Manchester, S.R., Dilcher, D.L., 1997. Reproductive and vegetative morphology of *Polyptera* (Juglandaceae) from the Paleocene of Wyoming and Montana. Am. J. Bot. 84, 649.
Manchester, S.R., Garden, M.B., 1987. The fossil history of the Juglandaceae. Ann. Mo. Bot. Gard. 21, 1–137.
Manning, W.E., 1978. The classification within the Juglandaceae. Ann. Mo. Bot. Gard. 1058–1087.
Martínez-García, P.J., Crepeau, M.W., Puiu, D., Gonzalez-Ibeas, D., Whalen, J., Stevens, K.A., Paul, R., Butterfield, T.S., Britton, M.T., Reagan, R.L., et al., 2016. The walnut (*Juglans regia*) genome sequence reveals diversity in genes coding for the biosynthesis of nonstructural polyphenols. Plant J. 87, 507–532.
Mattila, T.M., Bechsgaard, J.S., Hansen, T.T., Schierup, M.H., Bilde, T., 2012. Orthologous genes identified by transcriptome sequencing in the spider genus *Stegodyphus*. BMC genomics 13, 1.
McCormack, J.E., Hird, S.M., Zellmer, A.J., Carstens, B.C., Brumfield, R.T., 2013. Applications of next-generation sequencing to phylogeography and phylogenetics. Mol. Phylogenet. Evol. 66, 526–538.
Morris, G.P., Grabowski, P.P., Borevitz, J.O., 2011. Genomic diversity in switchgrass (*Panicum virgatum*), from the continental scale to a dune landscape. Mol. Ecol. 20, 4938–4952.
Moore, M.J., Soltis, P.S., Bell, C.D., Burleigh, J.G., Soltis, D.E., 2010. Phylogenetic analysis of 83 plastid genes further resolves the early diversification of eudicots. P. Natl. Acad. Sci. USA 107, 4623–4628.
Mu, Y.L., Xi, R.T., Lu, Z.R., 1990. Microsporogenesis observation and karyotype analysis of some species in genus *Juglans* L. J. Wuhan Bot. Res. 3, 301–310 (In Chinese).
Nicotra, A.B., Chong, C., Bragg, J.G., Ong, C.R., Aitken, N.C., Chuah, A., Lepschi, B., Borevitz, J.O., 2016. Population and phylogenomic decomposition via Genotyping-By-Sequencing in Australian *Pelargonium*. Mol. Ecol. 25, 2000–2014.
Ornelas, J.F., Gándara, E., Vásquez-Aguilar, A.A., Ramírez-Barahona, S., Ortiz-Rodriguez, A.E., González, C., Saules, M.T.M., Ruiz-Sanchez, E., 2016. A mistletoe tale: post-glacial invasion of *Psittacanthus schiedeanus* (Loranthaceae) to Mesoamerican cloud forests revealed by molecular data and species distribution modeling. BMC Evol. Biol. 16, 78.
Otto-Bliesner, B.L., Marshall, S.J., Overpeck, J.T., Miller, G.H., Hu, A., 2006. Simulating Arctic climate warmth and icefield retreat in the last interglaciation. Science 311, 1751–1753.
Perdereau, A., Klaas, M., Barth, S., Hodkinson, T.R., 2017. Plastid genome sequencing reveals biogeographical structure and extensive population genetic variation in wild populations of *Phalaris arundinacea* L. in north-western Europe. GCB Bioenergy 9, 46–56.
Phillips, S.J., Anderson, R.P., Schapire, R.E., 2006. Maximum entropy modeling of species geographic distributions. Ecol. Model 190, 231–259.
Posada, D., Crandall, K.A., 1998. Modeltest, testing the model of DNA substitution. Bioinformatics 14, 817–818.
Pollegioni, P., Woeste, K., Mugnozza, G.S., Malvolti, M.E., 2009. Retrospective identification of hybridogenic walnut plants by SSR fingerprinting and parentage analysis. Mol. Breeding 24, 321.
Pollegioni, P., Woeste, K., Chiocchini, F., Del Lungo, S., Ciolfi, M., Olimpieri, I., Tortolano, V., Clark, J., Hemery, G.E., Mapelli, S., Malvolti, M.E., 2017. Rethinking the history of common walnut (*Juglans regia* L.) in Europe: its origins and human interactions. PLoS One 12, e0172541.
Pollegioni, P., Woeste, K.E., Chiocchini, F., Olimpieri, I., Tortolano, V., Clark, J., Hemery, G.E., Mapelli, S., Malvolti, M.E., 2014. Landscape genetics of Persian walnut (*Juglans regia* L.) across its Asian range. Tree Genet. Genome 10, 1027–1043.
Pollegioni, P., Woeste, K.E., Chiocchini, F., Del Lungo, S., Olimpieri, I., Tortolano, V., Clark, J., Hemery, G.E., Mapelli, S., Malvolti, M.E., 2015. Ancient humans influenced the current spatial genetic structure of common walnut populations in Asia. PLoS One 10, e0135980.
Ronquist, F., Teslenko, M., van der Mark, P., Ayres, D.L., Darling, A., Höhna, S., Larget, B., Liu, L., Suchard, M.A., Huelsenbeck, J.P., 2012. MrBayes 3.2, efficient Bayesian phylogenetic inference and model choice across a large model space. Syst. Biol. 61, 539–542.
Rehder, A. 1940. Manual of cultivated trees and shrubs in North America. MacMillan Co., New York, USA.
Schlötterer, C., Tobler, R., Kofler, R., Nolte, V., 2014. Sequencing pools of individuals [mdash] mining genome-wide polymorphism data without big funding. Nat. Rev. Genet. 15, 749–763.
Schoener, T.W., 1968. The Anolis lizards of Bimini, resource partitioning in a complex fauna. Ecol. 49, 704–726.
Stanford, A.M., Harden, R., Parks, C.R., 2000. Phylogeny and biogeography of *Juglans* (Juglandaceae) based on *matK* and *ITS* sequence data. Am. J. Bot. 87, 872–882.
Stölting, K.N., Paris, M., Meier, C., Heinze, B., Castiglione, S., Bartha, D., Lexer, C., 2015. Genome-wide patterns of differentiation and spatially varying selection between postglacial recolonization lineages of *Populus alba* (Salicaceae), a widespread forest tree. New Phytol. 207, 723–734.
Wang, H., Pei, D., Gu, R.S., Wang, B.Q., 2008. Genetic diversity and structure of walnut populations in central and southwestern China revealed by microsatellite markers. J. Am. Soc. Hortic. Sci. 133, 197–203.
Wang, H., Pan, G., Ma, Q., Zhang, J., Pei, D., 2015. The genetic diversity and introgression of *Juglans regia* and *Juglans sigillata* in Tibet as revealed by SSR markers. Tree Genet. Genomes 11, 1–11.

Wang, W.T., Xu, B., Zhang, D.Y., Bai, W.N., 2016. Phylogeography of postglacial range expansion in *Juglans mandshurica* (Juglandaceae) reveals no evidence of bottleneck, loss of genetic diversity, or isolation by distance in the leading-edge populations. Mol. Phylogenet. Evol. 102, 255–264.
Warren, D.L., Glor, R.E., Turelli, M., 2008. Environmental niche equivalency versus conservatism, quantitative approaches to niche evolution. Evolution 62, 2868–2883.
Warren, D.L., Glor, R.E., Turelli, M., 2010. ENMTools, a toolbox for comparative studies of environmental niche models. Ecography 33, 607–611.
Wickham, H. 2009., ggplot2, elegant graphics for data analysis. Springer, New York.
Woodworth, R.H., 1930. Meiosis of microsporogenesis in the Juglandaceae. Am. J. Bot. 17, 863–869.
Wu, Y., Pei, D., Xi, K., 1999. Analysis of the origin and the taxonomic position of *Juglans hopeiensis* using RAPD markers. Scientia Silvae Sinicae 35, 25–30 (In Chinese).
Yang, Z., 2007. PAML 4, phylogenetic analysis by maximum likelihood. Mol. Biol. Evol. 24, 1586–1591.
Yang, X., Cheng, Y.F., Deng, C., Ma, Y., Wang, Z.W., Chen, X.H., Xue, L.B., 2014. Comparative transcriptome analysis of eggplant (*Solanum melongena* L.) and turkey berry (*Solanum torvum* Sw.), phylogenomics and disease resistance analysis. BMC genomics 15, 1.
Yang, J., Lee, S.H., Goddard, M.E., Visscher, P.M., 2011. GCTA, a tool for genome-wide complex trait analysis. Am. J. Hum. Genet. 88, 76–82.
Zhao, P., Woeste, K.E., 2011. DNA markers identify hybrids between butternut (*Juglans cinerea* L.), and Japanese walnut (*Juglans ailantifolia* Carr.). Tree Genet. Genomes 7, 511–533.
Zhang, J.B., Li, R.Q., Xiang, X.G., Manchester, S.R., Lin, L., Wang, W., Wen, J., Chen, Z.D., 2013. Integrated fossil and molecular data reveal the biogeographic diversification of the eastern Asian-eastern North American disjunct hickory genus (*Carya* Nutt.). PLoS One 8, e70449.